Geoscience Frontiers xxx (2015) 1–24

HOSTED BY

ELSEVIER

Contents lists available at ScienceDirect

China University of Geosciences (Beijing)

Geoscience Frontiers

journal homepage: www.elsevier.com/locate/gsf

Research paper

Comparison of mantle lithosphere beneath early Triassic kimberlite fields in Siberian craton reconstructed from deep-seated xenocrysts

I.V. Ashchepkov [a,*], S.S. Kuligin [a], N.V. Vladykin [b], H. Downes [c], M.A. Vavilov [a], E.N. Nigmatulina [a], S.A. Babushkina [d], N.S. Tychkov [a], O.S. Khmelnikova [a]

[a] Institute of Geology and Mineralogy SD RAS, Koptyug ave 3, Novosibirsk, Russia
[b] Institute of Geochemistry SD RAS, Favorskky str 1a, Irkutsk, Russia
[c] Department of Earth and Planetary Sciences, Birkbeck University of London, London, UK
[d] Institute of Geology of Diamonds and Noble metals SD RAS, Lenina ave 39, Yakutsk, Russia

ARTICLE INFO

Article history:
Received 27 August 2014
Received in revised form
4 June 2015
Accepted 15 June 2015
Available online xxx

Keywords:
Mantle lithosphere
Monomineral thermobarometry
Mineral geochemistry
Triassic kimberlite
Layering

ABSTRACT

Mantle xenocrysts from early Triassic kimberlite pipes from Kharamai, Ary-Mastakh and Kuranakh fields in the Anabar shield of Siberia revealing similar compositional trends were studied to estimate the superplume influence on the subcratonic lithosphere mantle (SCLM). Pressure-temperature (PT) reconstructions using monomineral thermobarometry for 5 phases show division of the SCLM beneath the Kharamai field into 6 units: pyroxenitic Fe-rich (1–2 GPa) and Mg-rich (2–3 GPa) layers; middle with two levels of Gar-Sp pyroxenites at ~3 and 4–5 GPa; Gar-dunite–harzburgites ~4.5–6.5 GPa subjected to Ilm-Px vein metasomatism; and a Mg-rich dunite lower part. In the Anabar shield (Ary-Mastakh, Dyuken and Kuranakh fields) mantle lithosphere is composed of three large units divided into two parts: upper part with amphiboles and phlogopite; two levels of pyroxenites and eclogites at 3 and 4 GPa, and a lower part composed of refertilized dunites. Diagrams showing P-Fe$^{\#}$Gar clusters for garnets and omphacites illustrate the differences between SCLM of these localities. Differences of Triassic SCLM from Devonian SCLM are in simple layering; abundance of Na-Cr-amphiboles and metasomatism in the upper SCLM part, thick pyroxenite-eclogite layer and lower part depletion, heated from SCLM base to 5.0 GPa.

Kharamai mantle clinopyroxenes represent three geochemical types: (1) harzburgitic with inclined linear REE, HFSE troughs and elevated Th, U; (2) lherzolitic or pyroxenitic with round TRE patterns and decreasing incompatible elements; (3) eclogitic with Eu troughs, Pb peak and high LILE content. Calculated parental melts for garnets with humped REE patterns suggest dissolution of former Cpx and depression means Cpx and garnets extraction. Clinopyroxenes from Ary-Mastakh fields show less inclined REE patterns with HMREE troughs and an increase of incompatible elements. Clinopyroxenes from Kuranakh field show flatter spoon-like REE patterns and peaks in Ba, U, Pb and Sr, similar to those in ophiolitic harzburgites. The PT diagrams for the mantle sections show high temperature gradients in the uppermost SCLM accompanied by an increase of P-Fe$^{\#}$Ol upward and slightly reduced thickness of the mantle keel of the Siberian craton, resulting from the influence of the Permian–Triassic superplume, but with no signs of delamination.

1. Introduction

The evolution of the subcratonic lithosphere mantle (SCLM) has been widely discussed (e.g. Pokhilenko et al., 1999; Griffin et al., 2003; Tappe et al., 2007; Santosh et al., 2009; Lee et al., 2011; Ashchepkov et al., 2013a,b,c,d). Most investigations suggest destruction of mantle keel over time because of hydration and weakening (Yu et al., 2011), subduction tension (Yang et al., 2012) or delamination due to plume influence (Li et al., 2015). The latter

* Corresponding author. United Institute of Geology and Mineralogy SD RASc, Academician V.A. Koptyug Avenue 3, 63090 Novosibirsk, Russia. Tel.: +7 9505918327; fax: +7 383 2332792.
E-mail addresses: Igor.Ashchepkov@igm.nsc.ru, igora57@mail.ru (I.V. Ashchepkov).
Peer-review under responsibility of China University of Geosciences (Beijing).

http://dx.doi.org/10.1016/j.gsf.2015.06.004

mechanism suggested for the Northern part of Siberian craton (Griffin et al., 2005) was taken for the explanation for the low diamond grade of post-Siberian superplume kimberlites. Here we compare mantle sections of early Triassic kimberlites to examine the possible influence of superplume on the SCLM.

The structure of the lithospheric mantle sequences beneath the Siberian craton was originally formed in the early–middle Archean time. Initially separate micro-continents formed in early–middle Archean terranes were probably joined together into a large continent, variably named Kenorland, Arctica or Superia-Sclavia (Williams et al., 1991; Bleeker, 2003; Santosh et al., 2009), assembling around 2.7 Ga marked by two peaks of zircon ages at 2.5 and 2.7 Ga (Griffin et al., 2014; Roberts and Spencer, 2015) and a peak in Re-Os model ages for sulfides at 2.8–2.7 Ga. The final accretion to Siberia took place at ~1.8–1.6 Ga (Rosen, 1986, 2003; Rosen et al., 2005, 2007). After the Mesoproterozoic break-up stage of Columbia, at 1.1–0.6 Ga Siberia became part of the next supercontinent Rodinia (Griffin et al., 2002; Pearson et al., 2005; Rosen et al., 2006; Mints, 2007; Maruyama et al., 2013). A preliminary study of mantle layering and compositions supports the idea of differences of subcontinental lithosphere mantle (SCLM) (Ashchepkov et al., 2013a) beneath each tectonic terrane in Siberia (Gladkochub et al., 2006).

Northern kimberlite fields in Yakutia are mainly Mesozoic and their SCLM xenoliths are much less studied than in the central parts of the craton. Siberian the Kharamai kimberlitic field (Fig. 1A) (Cherenkov et al., 1987) is located in the northwestern part of the Siberian craton, 250 km west of the southeastern part of the Anabar shield which belongs to the Magan terrane. This field relates to the early Triassic stage of kimberlitic magmatism of the Siberian platform as well as most kimberlites in the northern part of the Siberian craton (Kostrovitsky et al., 2007), including the regions of Anabar shield and Prianabarie (Brakhfogel, 1984; Kinny et al., 1997; Griffin et al., 1999a,b; Griffin et al., 2005; Rosen et al., 2005, 2006; Kostrovitsky et al., 2007; Smelov and Zaitsev, 2013). The exceptions are some Devonian kimberlites in Starorechenskoe, Toluopskoe and Ukukite fields and late Jurassic kimberlites like the Obnazhennaya pipe common in Kuoyka (Taylor et al., 2003) and some northern kimberlite fields (Moralev and Glukhovsky, 2000; Zaitsev and Smelov, 2010). Mesozoic kimberlites in Siberia are of low diamond grade but numerous diamond placers in the northern part of Siberian craton (Afanasiev et al., 2011) suggest undiscovered sources. Diamond inclusions from placers in Cir Anabar are essentially eclogitic (Sobolev et al., 1998; Shatsky et al., 2015) while in the central part of the Siberian craton (Logvinova et al., 2005) both peridotitic and eclogitic inclusions are common.

The compositions of minerals and structure of the Kharamai field were given by Griffin et al. (2005) based on previous explorations (Cherenkov et al., 1987). Wide distribution of the high-chromium pyropes (to 14 wt.% Cr_2O_3) in the kimberlites in this field and other northern parts of the Siberian platform, and pressure estimates of the xenoliths at ~5.1 GPa (Brey and Kohler, 1990) or 6.2 GPa (McGregor, 1974), as well as the abundance of diamond placers in the northern Prianabarie (Sobolev, 1974; Afanasiev et al., 2011), suggest that the mantle keel in the northern part of Siberian platform was similar in thickness to that in the central part of the Yakutian kimberlite province. This is supported by geophysical mantle profiles (Koulakov and Bushenkova, 2010; Pavlenkova, 2011; Kuskov et al., 2014). Nevertheless using pressure estimates for garnets (Ryan et al., 1996) it was assumed that the lower part of the lithospheric mantle in the northern part of Siberian craton was delaminated (Griffin et al., 2005) after the Siberian Permian–Triassic superplume event. However recent work suggests that it was only slightly reduced, mainly in Jurassic time (Howarth et al., 2014).

In this study the heavy concentrate minerals from three kimberlitic pipes of Kharamai field were used to determine the geochemistry of minerals and their parental melts and the structure of the SCLM in comparison with data obtained for kimberlites from some fields in the Anabar shield. Kharamai field is part of the Magan terrane (Gladkochub et al., 2006; Smelov and Zaitsev, 2013) as well as Mir pipe and the Malo-Botuobinsky kimberlite field. According to Rosen et al. (2006), the nearest Ary-Mastakh field belongs to the (West) Daldyn terrane similarly to the Alakit and Daldyn kimberlite fields. But according to more recent divisions this field Starorechenskoe, Duken and Kuranakh fields are situated within the Khapchan terrane as described by Zaitsev and Smelov (2010).

The mantle layering reconstructions and general geochemical characteristics of the minerals provide the typical features of the different terranes and their distinct parts (Ashchepkov et al., 2013a). By comparing the PTX$f(O_2)$ diagrams used for reconstructions of SCLM beneath the studied fields, we investigate the similarity of the mantle structure within the Magan terrane and differences with the SCLM in other tectonic units of the Siberian craton.

The geochemical characteristics of Kharamai field kimberlites are close to those of the Devonian kimberlites of Siberian platform (Kostrovitsky et al., 2007).

2. Data set and analytical methods

Mineral grains (~3100) of mantle xenocrysts of orthopyroxenes (Opx), clinopyroxenes (Cpx), garnets (Gar), olivine (Ol), chromite (Chr), ilmenite (Ilm) and amphiboles (Amph) from the Kharamai, Ary-Mastakh and Kuranakh kimberlites were analyzed in Analytic Centre of IGM SD RAN, Novosibirsk. Mostly the material was panned from the drilling mud.

Compositions of ~950 grains from three kimberlite pipes Evenkiyskaya, Malush and Tuzik from Kharamai field (Fig. 1B) were determined using the Jeol Superprobe electron microprobe (EMPA). In addition ~450 grains from the same pipes in Kharamai field, ~550 grains from Ary-Mastakh field (Fig. 1C) (Khardakh, Bumerang, Nebaibyt, Vympel and Bargadymalakh pipes) and ~1100 grains from Kuranakh field (Universitetskaya, Trudovaya, Losi, Malokuonamskaya pipes) (Fig. 1D) were determined using a CamebaxMicro electron microprobe (Ashchepkov et al., 2007, 2010) using 15 kV acceleration voltage and 15 nA beam current in epoxy mounts of the polished mineral grains according to the common procedure of Lavrent'ev and Usova (1994). For the constructions of the mantle transect we used additional data from some pipes in Duken field (Ashchepkov et al., 2001) and unpublished data for Malokounamskaya pipe provided by S. Babushkina and for the ilmenites from N.S Tychkov.

Minerals from Kharamai field (31), Ary-Mastakh field (Khardakh pipe, 17) and Kuranakh field (Universitetskaya, 9; Trudovaya, 20) pipe were analyzed by an LA-ICP-MS method using Finnigan Element I mass spectrometer with a Nd YAG 193: UV New Wave system laser. The laser spot diameter did not exceed 10–20 μm. Scanning time for each grain was about 2.5–3 min. The concentrations of 32 trace elements were obtained and normalized to ^{40}Ca using EPMA values for silicate minerals and to Ti and Cr for the ilmenites and chromites (Supplement 1).

3. Mineralogy

Pyropes of the Kharamai field, analyzed in this work, belong to the lherzolite field (Sobolev et al., 1973) reaching 11.5 wt.% Cr_2O_3 (Fig. 2A); reported values for the other pipes (Cherenkov et al., 1987; Griffin et al., 2005) are higher (14.5 wt.% Cr_2O_3).

Please cite this article in press as: Ashchepkov, I.V., et al., Comparison of mantle lithosphere beneath early Triassic kimberlite fields in Siberian craton reconstructed from deep-seated xenocrysts, Geoscience Frontiers (2015), http://dx.doi.org/10.1016/j.gsf.2015.06.004

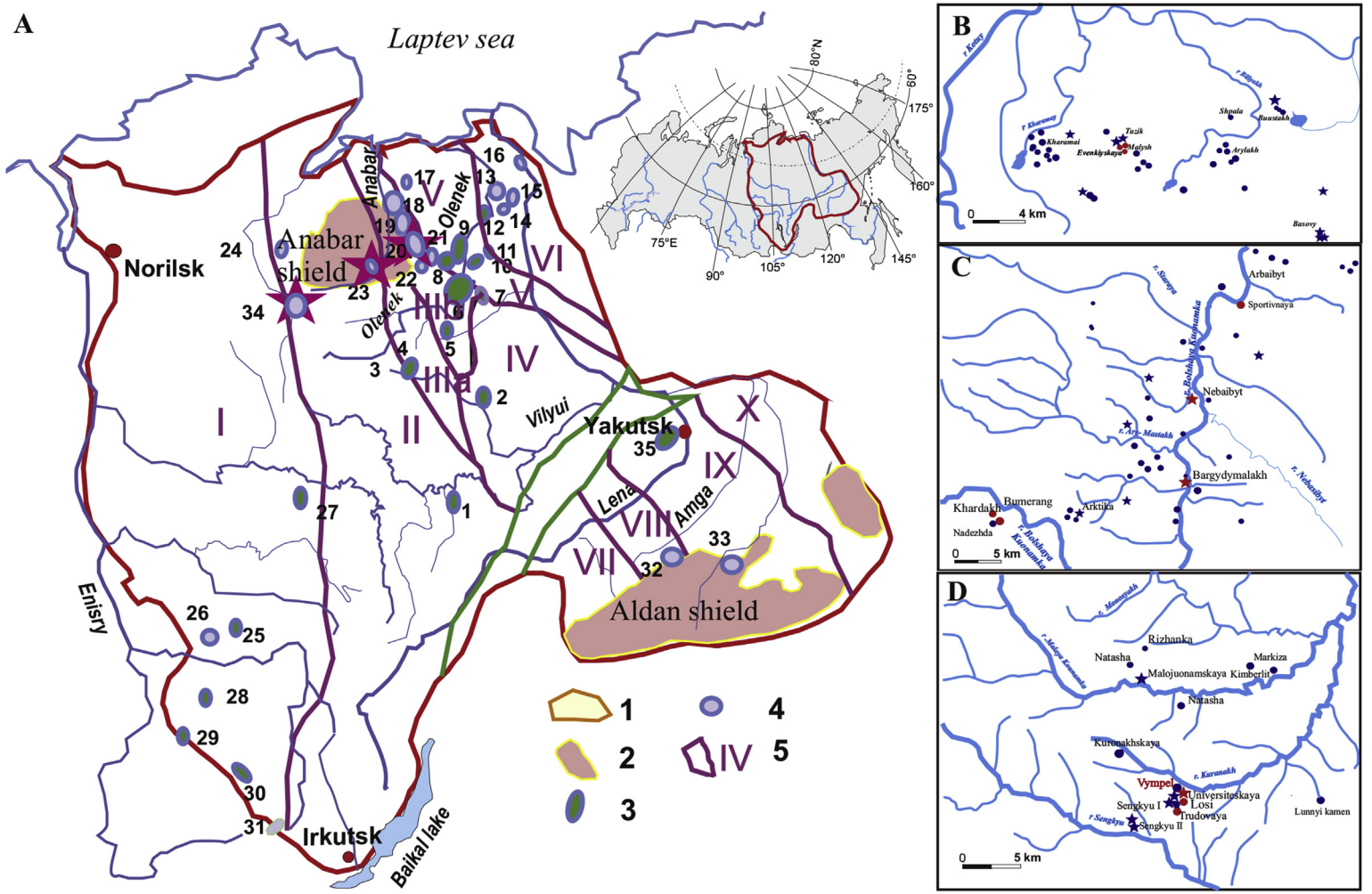

Figure 1. Scheme of the location for kimberlite and carbonatite fields (A) in Siberian platform, (B) in the Kharamai kimberlite field (Cherenkov et al., 1987), (C) in the Ary-Mastakh kimberlite field (Zaitsev and Smelov, 2010), (D) in the Kuranakh kimberlite field (Zaitsev and Smelov, 2010). 1–Siberian platform, 2–Shields, 3–Devonian kimberlites, 4–Triassic kimberlites, 5–Tectonic terranes. Fields: 1–Malo-Botuobinskoe, 2–Nakyn, 3–Alakit-Markha, 4–Daldyn, 5–Upper Muna, 6–Chomurdakh, 7–Severnei, 8–West Ukukit, 9–East Ukukit, 10–Ust-Seligir, 11–Upper Motorchun, 12–Merchimden, 13–Kuoyka, 14–Upper Molodo, 15–Toluop, 16–Khorbusuonka, 17–Ebelyakh, 18–Staraya Rechka, 19–Ary-Mastakh, 20–Dyuken, 21–Luchakan, 22–Kuranakh, 23–Middle Koupnamka, 24–Middle Kotui, 25–Chadobets, 26–Taichikun-Nemba, 27–Tychan, 28–Muro-Kova, 29–Tumanshet, 30–Belaya Zima, 31–Ingashi, 32–Chompolo, 33–Tobuk-Khatystyr, 34–Kharamai, 35––Manchary. The terranes are according to Glaldkochub et al. (2006), I–Tungus, II–Magan, IIIa–West Daldyn, IIIb–East Daldyn, IV–Markha, V–Khapchan, VI–Birekte, VII–XII: Aldan–Stanovoy province; VII–Olekma, VIII–Central Aldan, IX–East Aldan, X–Batomga.

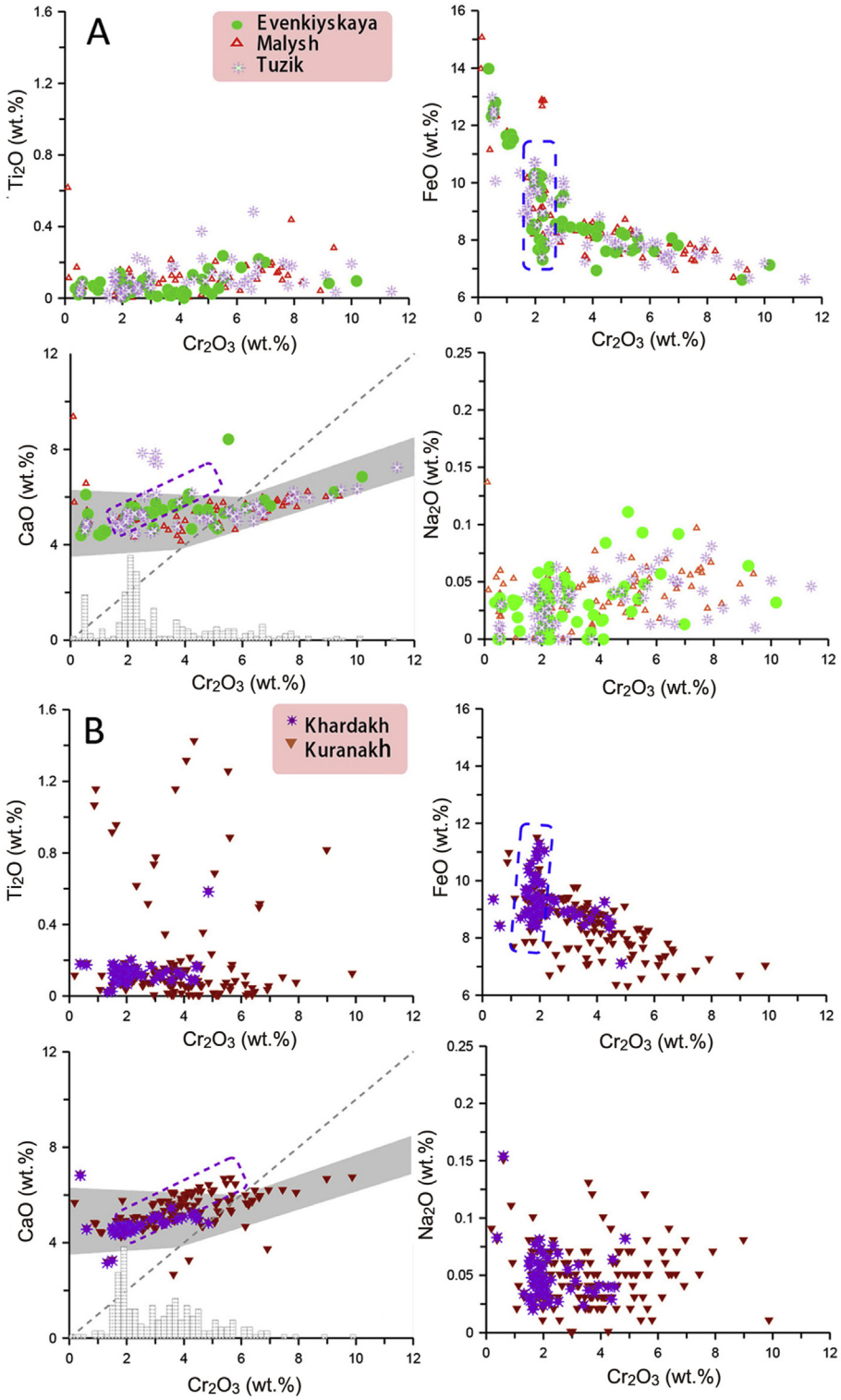

Figure 2. Variations of the garnet composition from the concentrate of the kimberlitic pipes of Kharamai field.

Pyroxenitic Ca-rich garnets are not frequent but the array from 1 to 4 wt.% Cr_2O_3 shows a CaO increase which is typical for Mesozoic kimberlite localities in Siberia (Ashchepkov et al., 2001; Tychkov et al., 2008) (Fig. 1). The dense cluster marked by elevated FeO values to 11 wt.% without high CaO should represent pyroxenites derived from basaltic melts. We did not find sub-calcic garnet and their amount determined in the concentrate earlier is small (Griffin et al., 2005). Garnets do not reveal considerable enrichment in TiO_2 (0.4 wt.%) and Na_2O (0.1 wt.%). Garnets from Khardakh pipe from the Ary-Mastakh field in Cr_2O_3-CaO plot show typical linear lherzolitic trend to 5 wt.% Cr_2O_3. Pyropes from the Kuranakh kimberlites are considerably enriched in TiO_2 (1.5 wt.%). They show inclined pyroxenitic trend from 1 to 6 wt.% Cr_2O_3. The continuation to 10 wt.% Cr_2O_3 with some amount of sub-calcic garnets (Fig. 2B) is

Please cite this article in press as: Ashchepkov, I.V., et al., Comparison of mantle lithosphere beneath early Triassic kimberlite fields in Siberian craton reconstructed from deep-seated xenocrysts, Geoscience Frontiers (2015), http://dx.doi.org/10.1016/j.gsf.2015.06.004

close to Paleozoic garnet trends. The eclogitic garnets as well as pyroxenitic were not considered for discussion because it is difficult to separate them from the lower crust granulitic species.

Clinopyroxenes from each of the Kharamai pipes are close in composition, although they differ in the dominant varieties (Fig. 3A). All together, the Cr-diopsides form two clouds in variation diagrams according to their FeO content. Pyroxenes with 1–2.5 wt.% FeO are characterized by the higher Cr_2O_3 (to 4 wt.%) content. The group of clinopyroxenes with elevated FeO (3–5 wt.%) is characterized by comparatively low Cr_2O_3 and higher Na_2O and

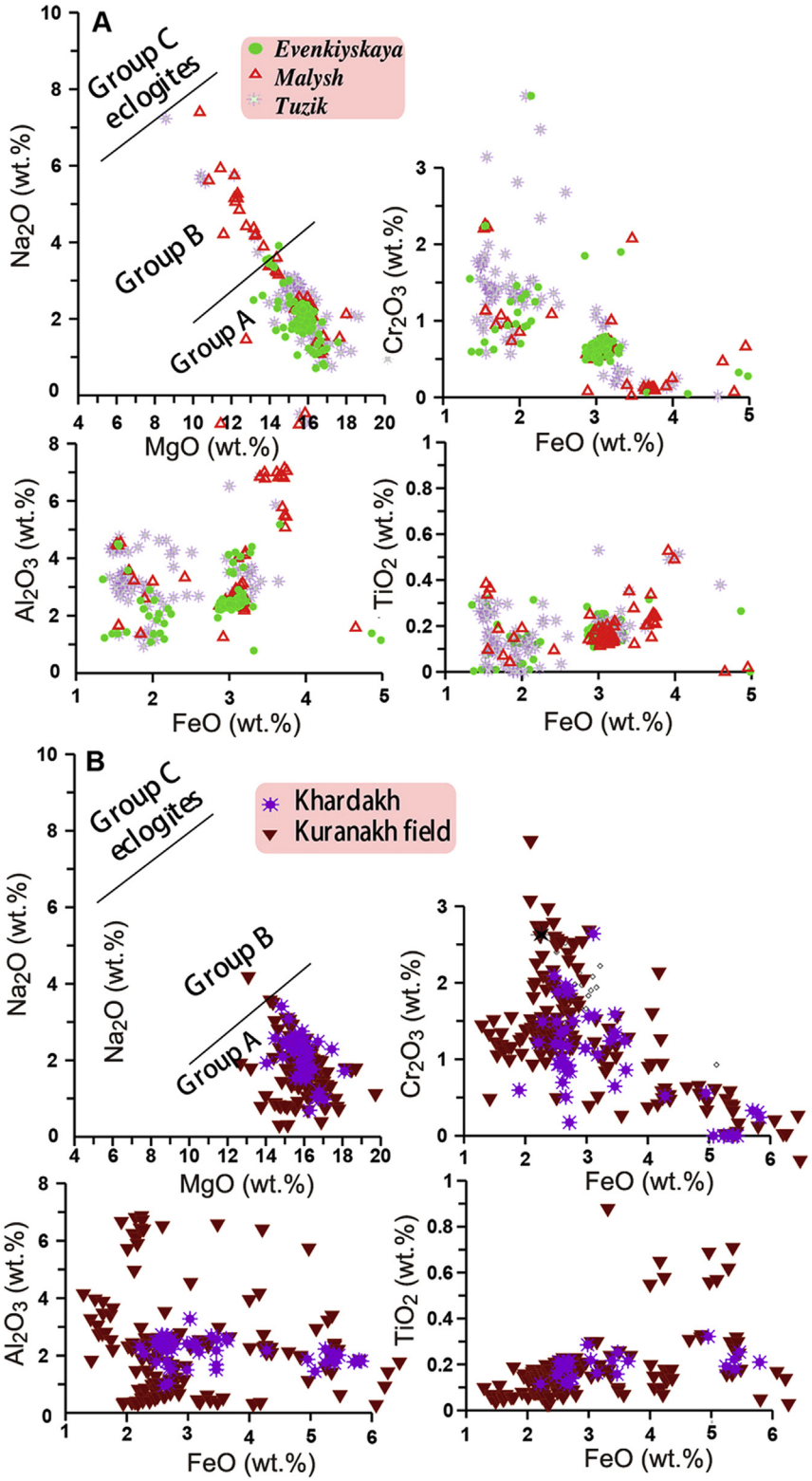

Figure 3. Variations of the clinopyroxene composition from the concentrate of the kimberlitic pipes of Kharamai field.

Please cite this article in press as: Ashchepkov, I.V., et al., Comparison of mantle lithosphere beneath early Triassic kimberlite fields in Siberian craton reconstructed from deep-seated xenocrysts, Geoscience Frontiers (2015), http://dx.doi.org/10.1016/j.gsf.2015.06.004

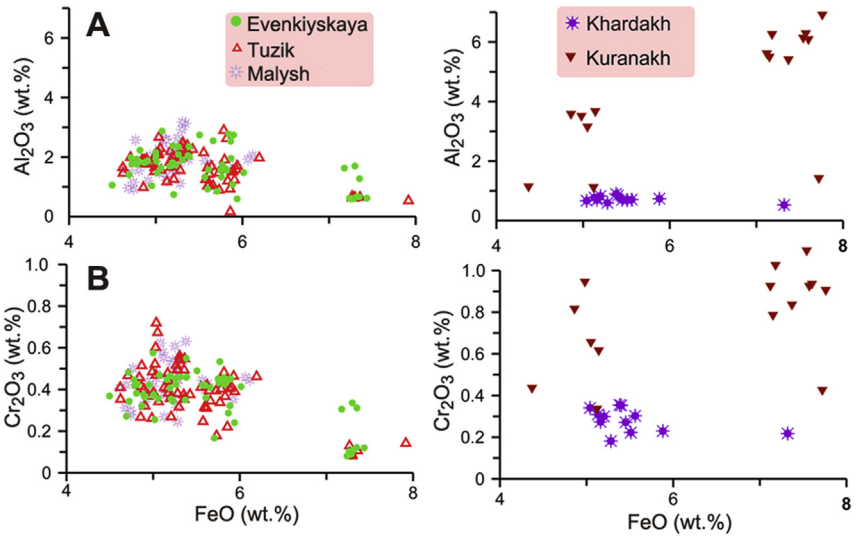

Figure 4. Variations of the orthopyroxene composition from the concentrate of the kimberlitic pipes of Kharamai field.

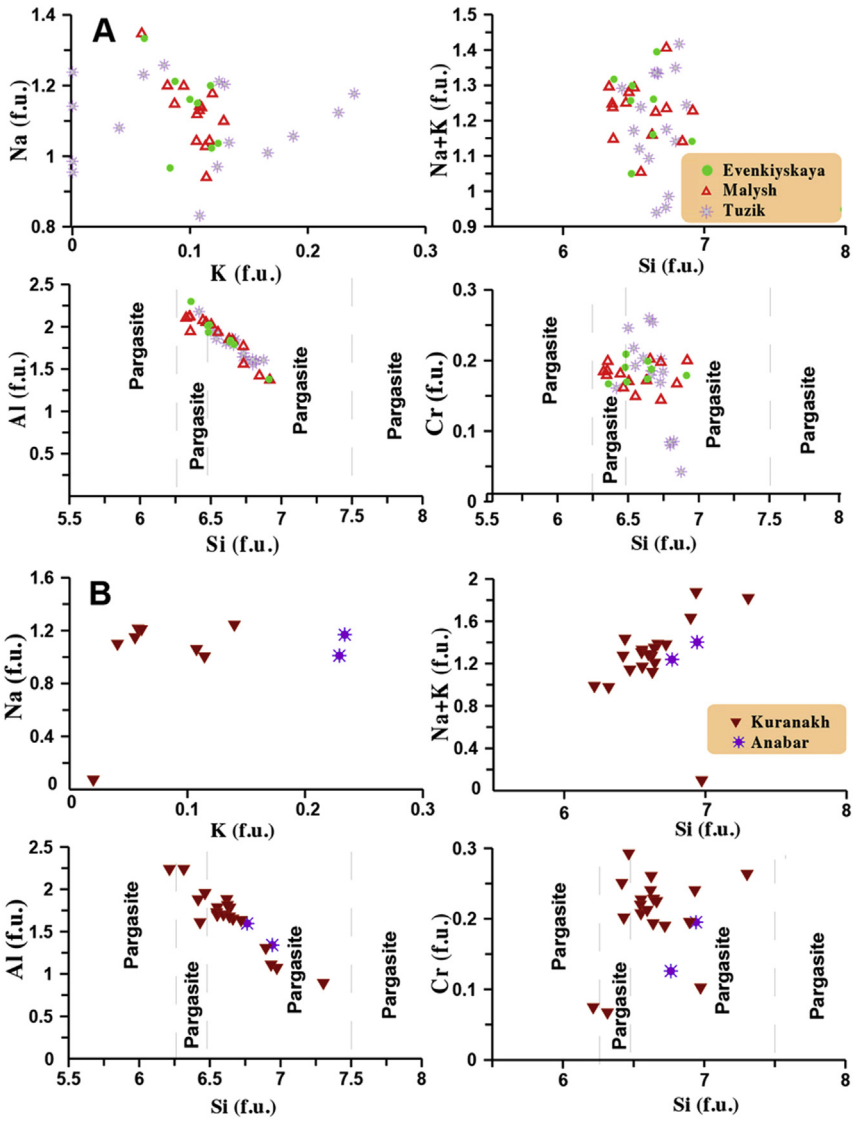

Figure 5. Variations of the amphiboles compositions from the concentrate of the kimberlitic pipes of Kharamai field.

Please cite this article in press as: Ashchepkov, I.V., et al., Comparison of mantle lithosphere beneath early Triassic kimberlite fields in Siberian craton reconstructed from deep-seated xenocrysts, Geoscience Frontiers (2015), http://dx.doi.org/10.1016/j.gsf.2015.06.004

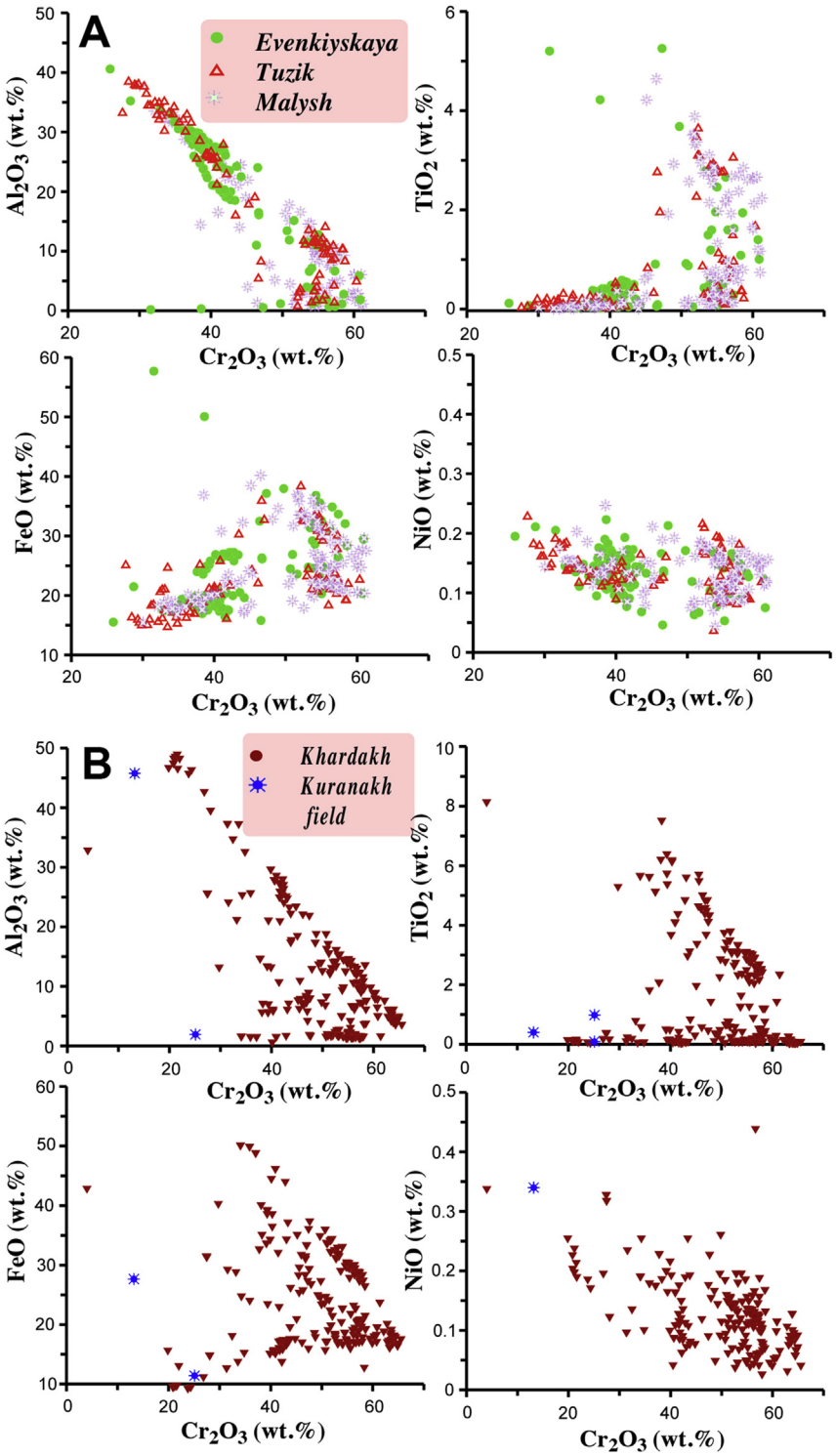

Figure 6. Variations of the chromite composition from the concentrate of the kimberlitic pipes of Kharamai field.

TiO_2 contents of some grains. Such values are common for pyroxene from Fe-rich metasomatites of the lithosphere base (Ionov et al., 2010; Ashchepkov et al., 2013a). Cr-diopsides from the Malysh pipe are more magnesian. Omphacites exist in concentrate from Malysh and much less in the Evenkiyskaya pipe, while from Tuzik pipe Cr-diopsides dominate.

Pyroxenes from the Anabar shield (Fig. 3B) show similar variations. The Na_2O content continuously increases together with FeO as in the Kharamai field but it decreases starting from 4.5 wt.% FeO.

Orthopyroxenes of Kharamai field are divided into two groups: magnesian with 4.5–6.2 wt.% FeO and ferrous >7.3 wt.% FeO. The first one reveals variations in Al_2O_3 from 1 to 3.5 wt.% and Cr_2O_3 for

Please cite this article in press as: Ashchepkov, I.V., et al., Comparison of mantle lithosphere beneath early Triassic kimberlite fields in Siberian craton reconstructed from deep-seated xenocrysts, Geoscience Frontiers (2015), http://dx.doi.org/10.1016/j.gsf.2015.06.004

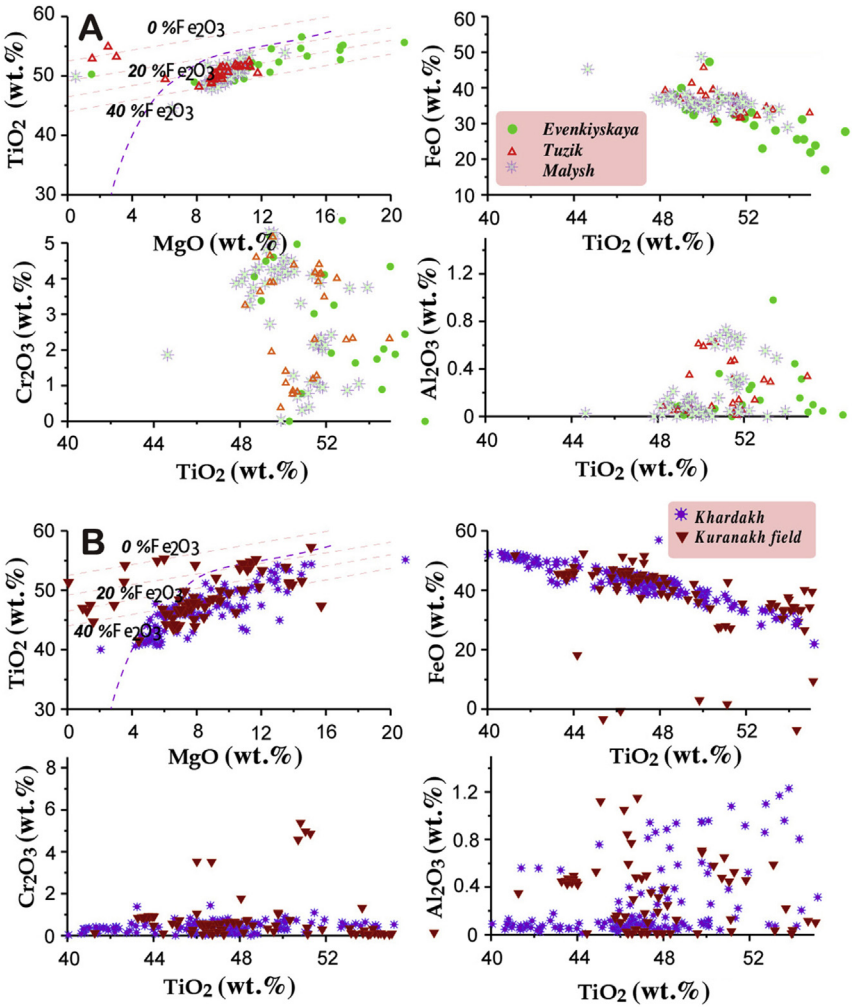

Figure 7. Variations of the ilmenite composition from the concentrate of the kimberlitic pipes of Kharamai field.

0.2–0.8 wt.% with small TiO_2 fluctuations (Fig. 4A). Al-Fe-enriched varieties are from pyroxenes especially in CaO. Orthopyroxenes in kimberlites from Anabar shield (Fig. 4B) are mostly found in Khardakh pipe and are rare in other pipes. They show very close intervals of $Fe^{\#}$ but reveal higher variations in CaO, TiO_2, Al_2O_3 and Cr_2O_3.

Amphiboles of the Kharamai field are mostly Cr-hornblendes. We used division of amphiboles after Leake et al. (2003). The K-Na in formula units (f.u.) negative isomorphic trend is typical only for magnesian varieties (Fig. 5A). The Fe-enrichment is accompanied by the joint increases in Fe, Na, K_2O, TiO_2 and Al_2O_3 and Cr_2O_3 decreases. Amphiboles of the Anabar shield (Fig. 5B) reveal similar regularities but smaller variations.

Chromites and Cr spinels from the Kharamai field are divided into two large groups (Fig. 6A). The most Cr-rich (65–50 wt.% Cr_2O_3) varieties are enriched by an ulvospinel component in different degree (to 6 wt.% TiO_2) accompanied by the rise of FeO to 40 wt.%. Simultaneous increase in Cr_2O_3, V_2O_5 and decrease in Nb_2O_5 is observed. Insignificant decline for NiO is found for middle part of Cr_2O_3 trend. Similar trends but extending further to the Al-rich part are determined for the chromites from the Ary-Mastakh (Fig. 6B) and Kuranakh fields. Reduction in Cr_2O_3 is accompanied by the splitting of FeO trends and by the increase in NiO and decrease in MnO.

Ilmenites of the Kharamai field reveal a narrow TiO_2 range and complex variation trends for most components (Fig. 7A). Decrease in TiO_2 from 56 to 48 wt.% is accompanied by an increase in Cr_2O_3 typical for metasomatic associations. There are also varieties without Cr derived from the primitive proto-kimberlite melts which did not interact with peridotites. The Al_2O_3 and V_2O_5 admixtures as well as Nb_2O_5 and ZnO increase with TiO_2 decreasing. Higher amount of the ilmenites and wider compositional variation is detected for the Tuzik kimberlite.

Ilmenites from the kimberlite from the Kuranakh field (Fig. 7A) reveal a continuous compositional range from 40 to 55 wt.% TiO_2. The Cr content of picroilmenite xenocrysts in the Khardakh pipe is much lower in comparison to those from the Kharamai field, but several ilmenites of the Kuranakh field show Cr_2O_3 contents up to 5 wt.%. The NiO content is comparatively low, whereas V_2O_5 and Al_2O_3 concentrations are much lower.

4. Variations of the trace elements in minerals

Garnets from the Kharamai pipes are divided into 3 groups according to their trace element (TRE) patterns (Fig. 8A) (Supplement 1). The first (Gr1) is characterized by round patterns with the domination of HREE and smooth decrease of LREE. For the second group (Gr2) the significant hump in MREE with the center near Sm is probably the sign of pyroxenite assemblage (Ashchepkov et al., 2011) (see discussion). For the third group (Gr3) lower HREE and the small minimum in Dy-Er is common and a sign of harzburgitic garnets (and some pyroxenes). Most garnet spider diagrams reveal high maximums of Pb, U and substantial Ta increase relative to Nb which is higher for the LREE-enriched varieties as commonly found

Please cite this article in press as: Ashchepkov, I.V., et al., Comparison of mantle lithosphere beneath early Triassic kimberlite fields in Siberian craton reconstructed from deep-seated xenocrysts, Geoscience Frontiers (2015), http://dx.doi.org/10.1016/j.gsf.2015.06.004

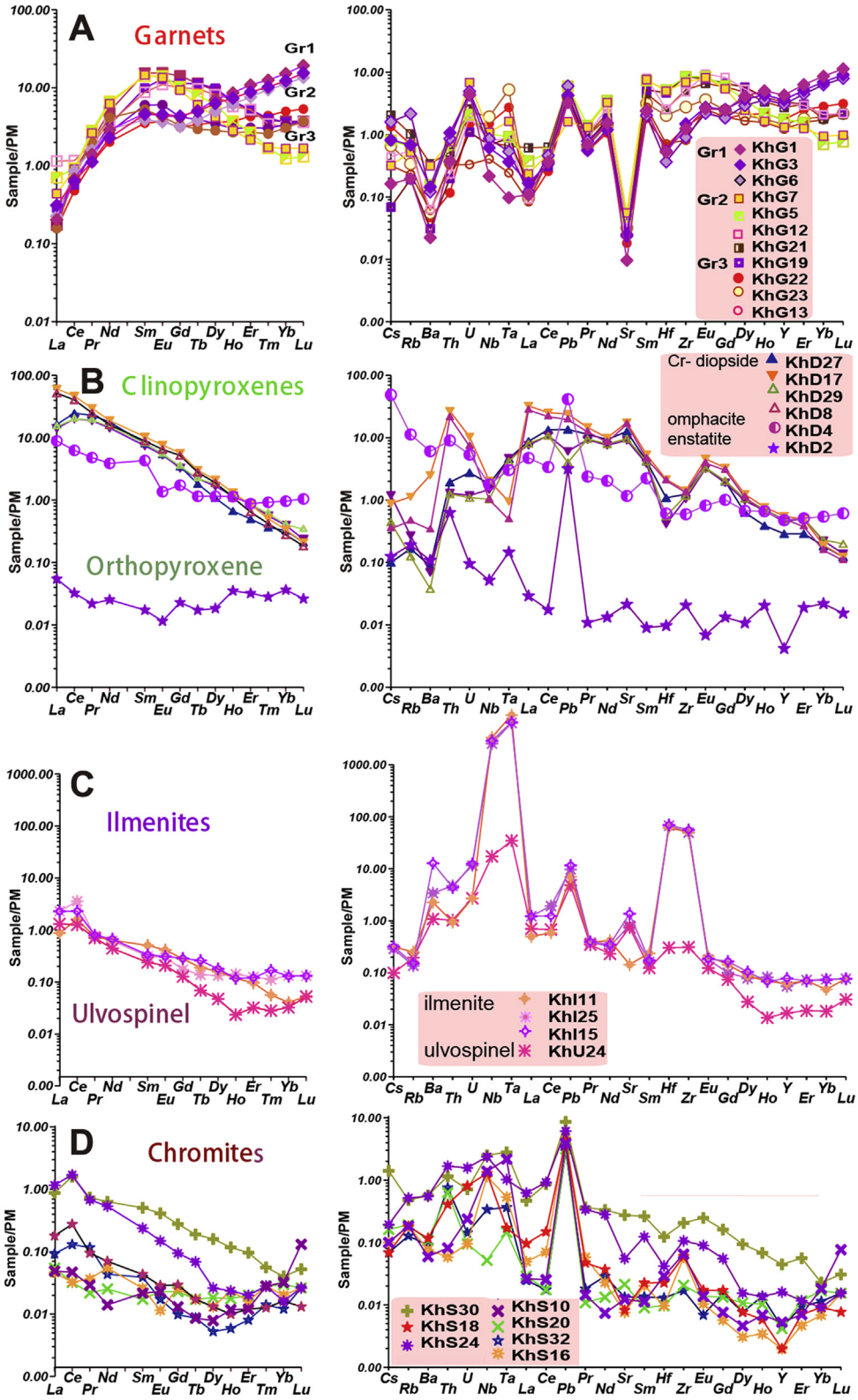

Figure 8. REE patterns and TRE spidergrams for deep seated xenocrysts from the Kharamai kimberlite field.

for the metasomatic varieties (Gregoire et al., 2003). The general TRE exhaustion is accompanied by Ta < Nb and rises of Zr/Hf_n ratios which is found for the carbonatite melts (Nelson et al., 1988; Andrade et al., 2008). All types of garnets show troughs in Sr, Ba and a varying Zr minimum.

Clinopyroxenes from the Kharamai kimberlites show three types of TRE spider diagrams. Varieties with the highly inclined linear REE patterns and MHREE depression most likely relate to the garnet harzburgite type as those from the Alakit field in Central Yakutia (Ashchepkov et al., 2004). They have minima at Nb, Ta and

Please cite this article in press as: Ashchepkov, I.V., et al., Comparison of mantle lithosphere beneath early Triassic kimberlite fields in Siberian craton reconstructed from deep-seated xenocrysts, Geoscience Frontiers (2015), http://dx.doi.org/10.1016/j.gsf.2015.06.004

smaller depressions in Zr-Hf. The peaks in Th, U are typical for carbonatite melts (Fig. 8B) (Andrade et al., 2008). The pattern with Eu minimum and peak at Pb and high content LILE belongs to eclogitic type.

The single analyzed orthopyroxene revealed a smooth increase in all incompatible components, peaks in Pb, Th, and Y minimum, which refers to Al-poor rocks.

Most ilmenites show gently inclined REE patterns with LREE levels ~5 orders of magnitude higher relative to primitive mantle (PM) (McDonough and Sun, 1995). The high peaks in Nb, Ta, and Zr are characteristic for other kimberlitic ilmenites (Ashchepkov et al., 2012; Afanasiev et al., 2013). These peaks become lower for ilmenites with lower TiO_2 content having small depressions in Dy-Tm. The last two elements are considerably lower for the varieties which show slightly U-shaped REE patterns (Fig. 8C).

Chromites reveal REE patterns of two types. Those exhausted in REE have convex spoon-like patterns with minima in HREE, small Y trough, and peaks in Pb, Nb, Ta and Th. For the relatively enriched chromites, a decrease of the incompatible elements is observed (Fig. 8D).

Clinopyroxenes from the Khardakh pipe (Fig. 9A) (Supplement 1) show two major types of TRE diagrams. The first one refers to the typical Cr-diopsides showing more LREE enriched patterns with the higher $(La/Yb)_n$ ratios and relatively smaller depression in Ta-Nb and trough in Zr. The Fe-rich pyroxenes and transitional pyroxenes show lower La/Yb ratios and complex REE patterns consisting from two branches divided by inflections and minima in En. The flatter HREE part shows small depressions from Tm to Ho. The spidergrams of these clinopyroxenes reveal increase in Th, U, Pb and deep minima at Nb and Ta, sometimes decoupled but with even elevation in Zr and Hf. The more Fe-rich pyroxenes have deeper Eu minimums and higher difference in high field strength elements (HFSE). They are pyroxenitic pyroxenes showing rather low Na-Al content.

Inclined (for those enriched in REE) or concave downward patterns (for those exhausted in REE) are determined for ilmenites

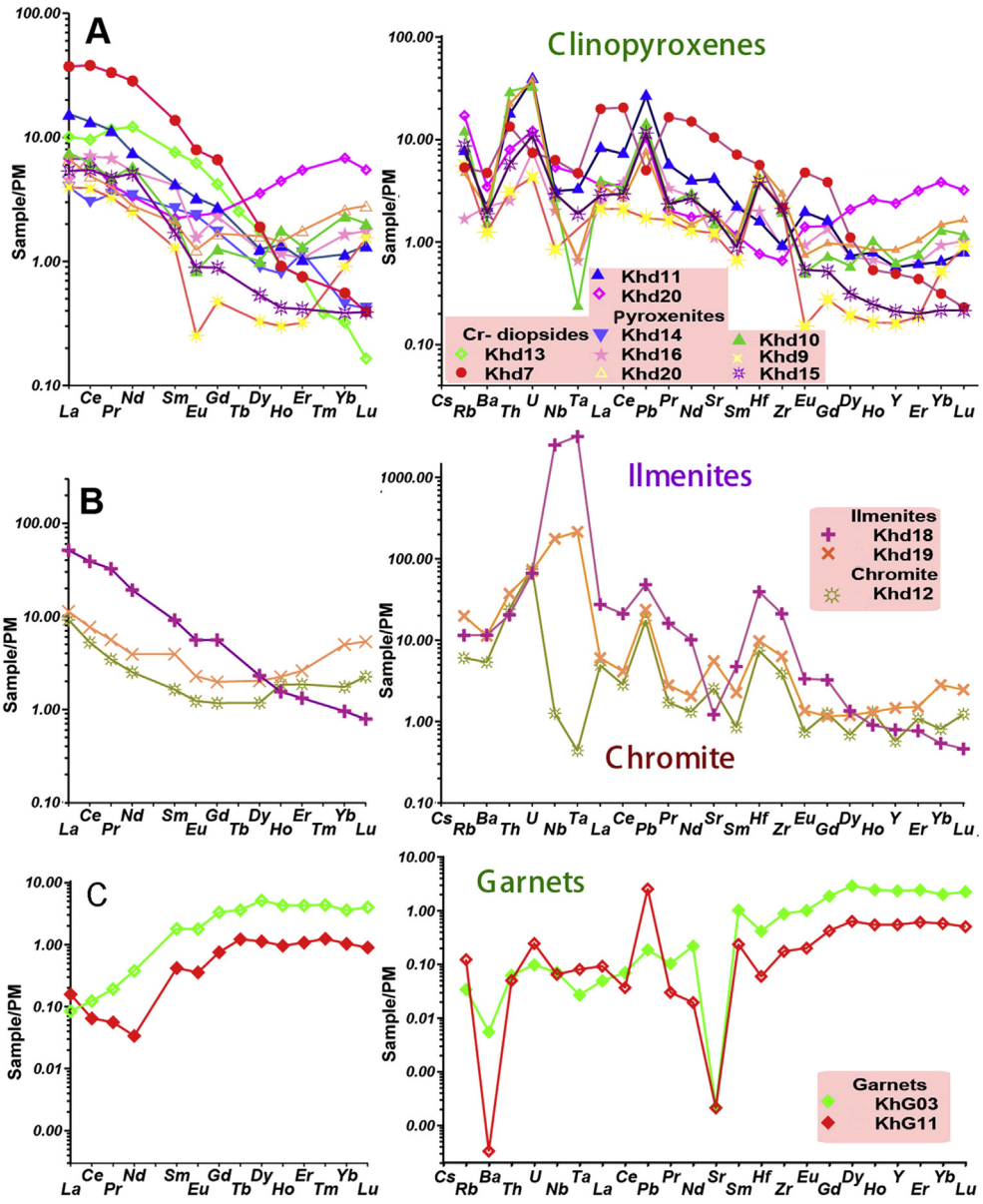

Figure 9. REE patterns and TRE spidergrams for deep seated xenocrysts from the Khardakh kimberlite pipe, Ary-Mastakh field.

Please cite this article in press as: Ashchepkov, I.V., et al., Comparison of mantle lithosphere beneath early Triassic kimberlite fields in Siberian craton reconstructed from deep-seated xenocrysts, Geoscience Frontiers (2015), http://dx.doi.org/10.1016/j.gsf.2015.06.004

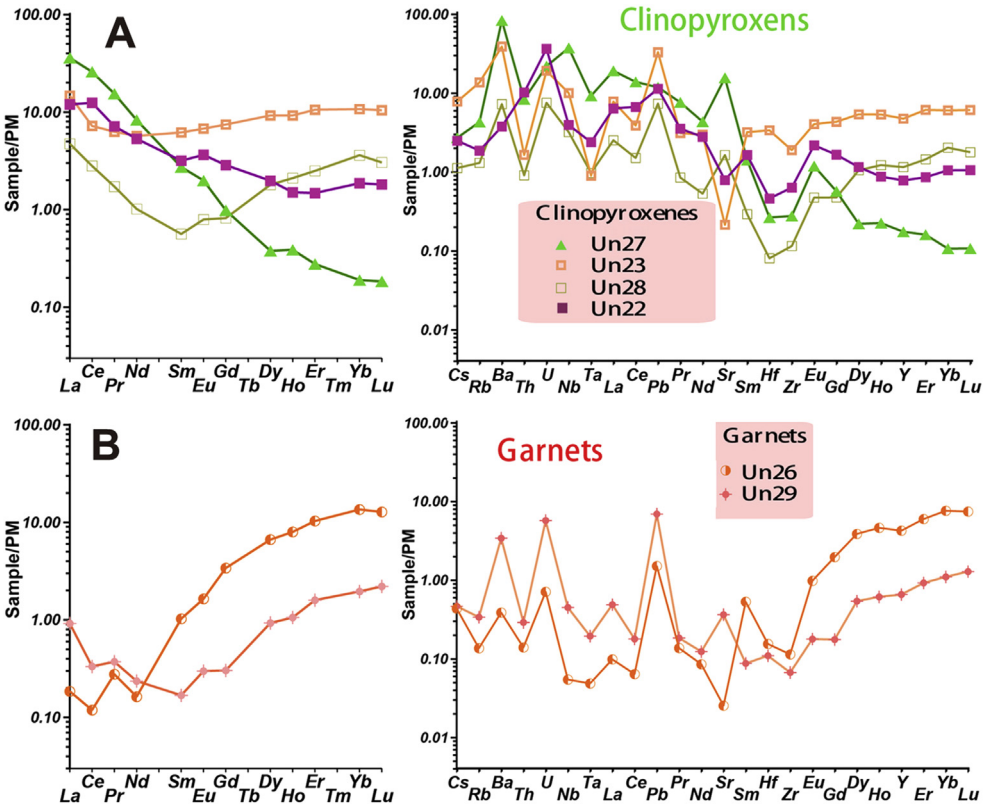

Figure 10. REE patterns and TRE spidergrams for the melt parental for the minerals from deep seated xenocrysts from the kimberlite pipes Universitetskaya pipe of Kuranakh field.

from the Kharamai kimberlites. All ilmenite spider diagrams have strong Ta, Nb and smaller Zr, Hf peaks which are typical for metasomatic associations, for example in Sytykanskaya pipe from Alakit fields (Ashchepkov et al., 2004). In this pipe, the ilmenites are characterized by enrichment in U and HFSE. Chromite patterns show a Ta-Nb trough instead of peaks (Fig. 9B).

In the Universitetskaya pipe from the Kuranakh field, low-Cr garnets have flatter REE patterns like those from the Khardakh pipe. However, chromium pyrope reveals typical rounded REE patterns with minima in Sr and peaks in U, Pb, Ba and minima in Nb, Ta, Zr and Hf (Fig. 10) which are characteristic for harzburgites or lherzolites of subduction-type. Clinopyroxenes from this pipe have similar REE spoon-like in LREE or U-shaped patterns as detected for pyroxene from garnet-spinel or spinel mantle facies (Dantas et al., 2009). Two pyroxenes have inclined patterns which are commonly found in garnet-bearing harzburgites. Despite differences in REE they show more uniform TRE behavior. The peaks in U, Ba or the opposite distinct minima in Pb and less pronounced in Th, Ta, Zr are observed in the spider diagrams.

Clinopyroxenes from the Trudovaya pipe (Fig. 11A) reveal more uniform highly inclined pattern with a different level of REE. The most enriched spider diagrams have small peaks in Eu, Ce minima and a deep Pb trough which probably reflects an admixture of eclogitic material. In the TRE spiderdiagram the Rb peaks and small minima of HFSE and more expressed in Th, Ba are observed.

Ilmenites have two types of TRE spider diagrams. Varieties with the low TRE concentrations possess inclined REE patterns and well expressed peaks in Ta, Nb Zr-Hf and Pb. They are characterized by minima in Sr and large ion lithophile (LILE) elements. Ilmenites with the LREE level ~100–1000 enriched relative to primitive mantle show inclined REE patterns and the minimums in Pb, Sr. The peaks in Nb, Ta, Zr and Hf are not as strong as in previous ilmenite group.

5. Thermobarometry

5.1. PTXf(O_2) conditions beneath Kharamai field and Prianabarie

The methods of monomineral thermobarometry (McGregor, 1974; O'Neill and Wood, 1979; Nimis and Taylor, 2000; Ashchepkov et al., 2010) combined in thermobarometric program (Supplement 2) in the application for five minerals from the concentrate of three pipes from Kharamai field and kimberlites from Prianabarie were used for reconstructing of sections of SCLM beneath Kharamai and Anabar kimberlitic fields Prianabarie for the same early Triassic stage of kimberlite magmatism.

A combined diagram for the mantle section beneath the Kharamai field based on mantle xenocrysts of three pipes together shows division into 6 (according to garnet clusters) or 3 large units and pressure (Fig. 12). The pyroxenes and garnets mark different geothermal branches which is typical for mantle sections (Fraser and Lawless, 1978). The Moho boundary is fixed by the PT estimates for the eclogitic omphacites and pyroxenites. The stratigraphic levels from 3.5 to 2.5 and then to 1 GPa in the upper part of the SCLM most likely correspond to garnet pyroxenites and lherzolites. The garnet-spinel pyroxenite lens showing elevated Fe occurs in the 1–2 GPa interval. The heated eclogites–pyroxenites are located at the level close to 2.5–3 GPa. But low temperature eclogites belong to the 3.5–4 GPa interval, which marks the boundary between upper and lower parts of mantle lithosphere. It is traced also by the peridotites rich in pyroxenes showing highest temperature (HT) and low temperature (LT) conditions. A similar layer has been detected beneath the Udachnaya (Pokhilenko et al., 1999), Mir

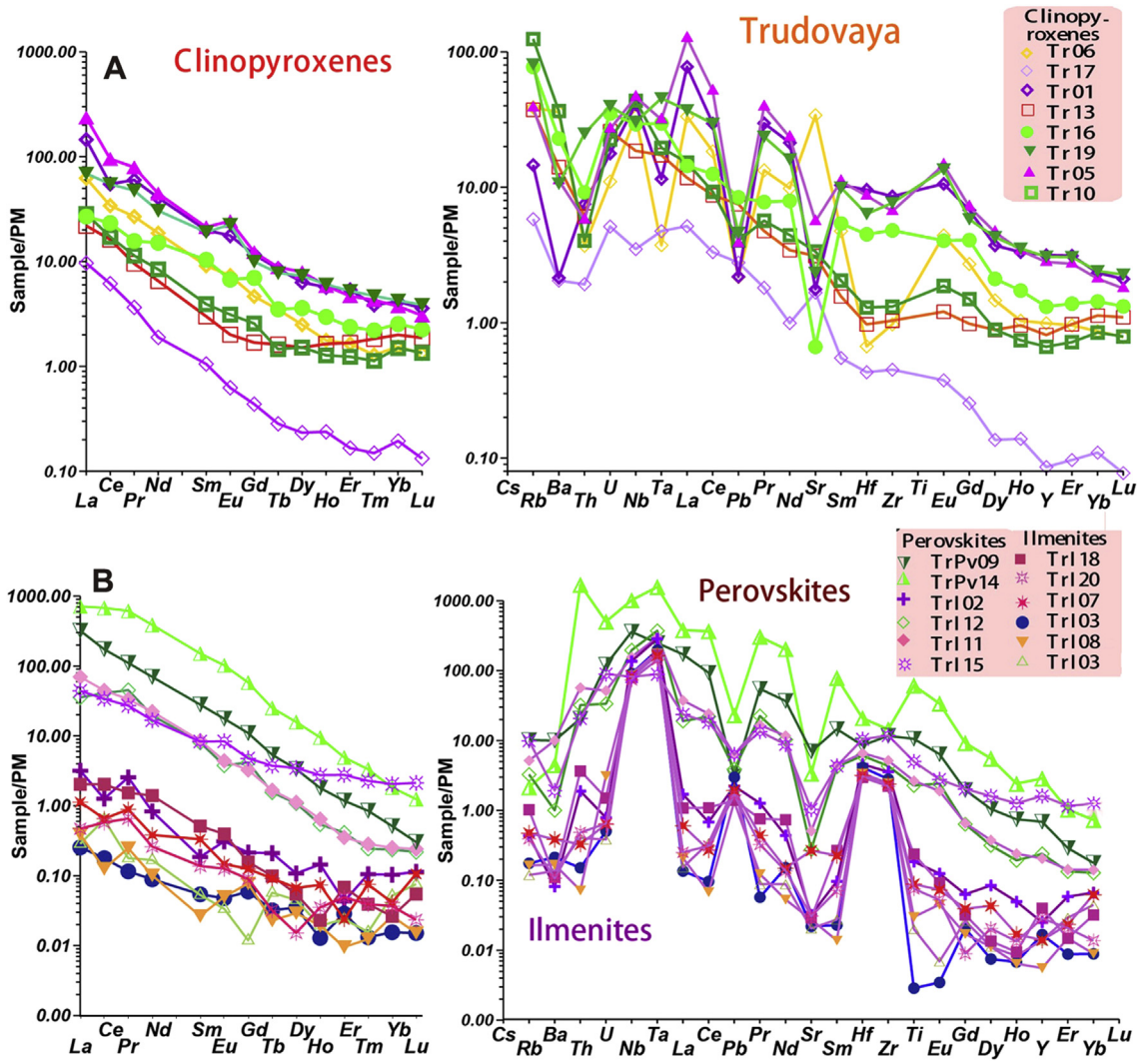

Figure 11. REE patterns and TRE spidergrams for the melt parental for the minerals from deep seated xenocrysts from the kimberlite pipes Trudovaya pipe of Kuranakh field.

(Ashchepkov et al., 2010, 2013a,b) pipes and in other regions. Deeper in the range from 5.0 to 3.5 GPa, the joint PT estimates for garnets and ilmenites indicate the presence of metasomatic ilmenite peridotites, judging by the agreement of calculations of $Fe^{\#}$ in Ol equilibrated with ilmenites and garnets. The low-Cr ilmenites fix proto-kimberlitic magma chambers or dense channels at this level created during protokimberlite magma ascent, similar to the processes of megacryst growth in alkali basalts (Ashchepkov et al., 2011). The lower sub-lens in 6.5–5 GPa interval is composed mostly of pyroxenites or wehrlite type with Ca-rich garnets. Coinciding PT estimates of Ti-chromites and Cr-bearing ilmenite suggest that they should be from the intergrowths found in Nebaibut pipe. The megacrystalline association is represented by low-Cr ilmenites, ortho- and clinopyroxenes.

Concentrates from each pipe reveal the same division of the mantle section slightly varying in compositions of minerals and fraction of the minerals in the concentrate, as it was determined for kimberlites from Angola (Ashchepkov et al., 2012). The concentrate from the Tuzik pipe contains more ilmenites and eclogites. The high temperature branch is more pronounced, starting from 4 GPa to the top of the mantle section.

The SCLM beneath the Evenkiyskaya pipe in general reveals characteristics that are found in the combined diagram (Supplement 3, Fig. 1A). But the amount of Cr-rich garnets is less than in concentrates from other pipes. In the mantle section beneath Malysh pipe (Supplement 3, Fig. 1B), the amount of chromites forming 3 clusters in SCLM is much higher than beneath the others. In contrast the amount of picroilmenites is higher but eclogitic omphacites are lower in SCLM beneath the Tuzik pipe (Supplement 3, Fig. 1C).

The conductive 37 mWm^{-2} geotherm (Mather et al., 2011) is traced mainly by garnet PT estimates in SCLM beneath the Kharamai pipe field. The clinopyoxene geotherm (Grutter, 2009) especially determined by Nimis and Taylor (2000) method give as usual lower temperature conditions (Nimis et al., 2009). There are no evidences about sheared peridotites showing HT branches and Fe-Ti-Na increasing trend for pyroxenes (Nixon and Boyd, 1973). The highest pressure values for ilmenites, rare garnets and clinopyroxenes are close to 7.5 GPa. It is possible that the mantle lithosphere in this region was thicker before the Permian–Triassic heating as was suggested in previous works (Griffin et al., 2005; O'Reilly and Griffin, 2010; Howarth et al., 2014).

The reconstructed mantle column beneath the Khardakh pipe in Ary-Mastakh field also contains 3 large clearly expressed units (Fig. 13A), with subdivision of each into 2 layers. In the upper part from 3 to 1 GPa, Fe-garnet peridotites and pyroxenites prevail. A

Please cite this article in press as: Ashchepkov, I.V., et al., Comparison of mantle lithosphere beneath early Triassic kimberlite fields in Siberian craton reconstructed from deep-seated xenocrysts, Geoscience Frontiers (2015), http://dx.doi.org/10.1016/j.gsf.2015.06.004

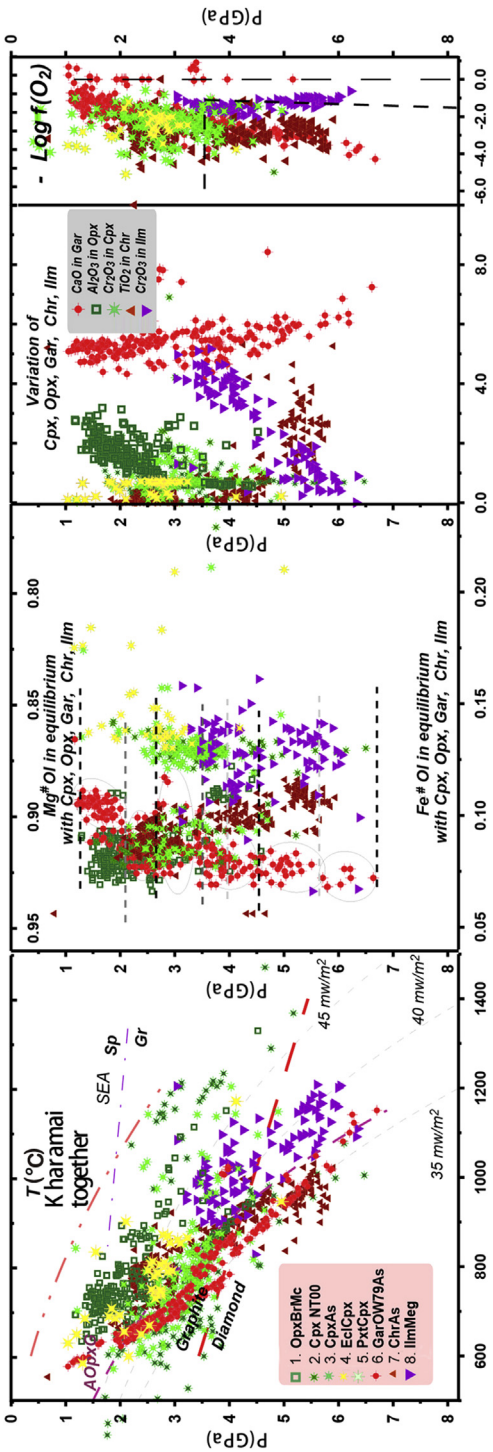

Figure 12. PTX$f(O_2)$ diagram for the minerals from the concentrates of the kimberlite pipes from Kharamai field together. The symbols: 1. Opx, T (°C) (Brey and Kohler, 1990) - P (GPa) (McGregor, 1974); 2. Cpx, T (°C) (Nimis and Taylor, 2000) - P (GPa) (Ashchepkov et al., 2010) for peridotites; 3. T (°C)-P (GPa) (Nimis and Taylor, 2000) for peridotites; 4. T (°C) (Nimis and Taylor, 2000) - P (GPa) (Ashchepkov et al., 2010) for the eclogite; 5. the same for the pyroxenite; 6. garnet (monomineral), T (°C) (O'Neill and Wood, 1979) - P (GPa) (Ashchepkov et al., 2010); 7. Chromite, T (°C) (O'Neill and Wall, 1987) - P (GPa) (Ashchepkov et al., 2010); 8. Ilmenite, T (°C) (Taylor et al., 1998) - P (GPa) (Ashchepkov et al., 2010).

small pyroxene-rich lens is present at the level ~2.5 GPa. Substantially pyroxenitic lens in the middle part (3–4.5 GPa) is thermally heterogeneous. The highest heating and elevating Fe# values within 4–3.5 GPa refer to the eclogitic compositions. Clinopyroxene-bearing rocks became low-temperature near 5 GPa. The inflection of the geothermal gradient corresponding to the appearance of the so-called convective branch is marked by the orthopyroxenes, and ilmenites PT estimates near 5–6.5 GPa. The orthopyroxene-clinopyroxene ilmenite-bearing peridotites and heated garnet peridotites of low Fe# are located below this boundary.

The ilmenite P-Fe# trend with the continuous increase in Fe# from 6 to 3 GPa shows division to three parts. In the lower part of the section in the 7–6 GPa interval, relatively low Fe# ~0.1 corresponds to the Opx estimates and the low pressure part Fe#Ol for ilmenites is close to the clinopyroxenes PT points near 0.18.

Mantle sequences beneath the Kuranakh field show division into 3 major units with further subdivisions (Fig. 13B). In the upper part the minerals from peridotites and pyroxenites show the increase of Fe# near the Moho. This part of the section is very heated up to 90 mW/m^2 (SEA geotherm). This is common for alkali basalt inclusions. In the interval of 3–4 GPa it is possible to recognize several linear trends of increased Fe# with decreasing pressure which is common for differentiating melts. The oxidation state of the peridotites of the upper part of SCLM beneath the Khardakh pipe is more heterogeneous in the upper SCLM part.

Below the level of 4.0 GPa in the section, chromite-bearing dunites should dominate. Sometime they contain garnet nests or lenses (Ashchepkov et al., 2001). These rocks are found as kimberlite xenoliths in the Dyuken and Ary-Mastakh fields in core from some boreholes (Ashchepkov et al., 2001). They are not similar to the diamond-bearing megacrystalline dunites with the subcalcic garnets from the center of the craton (Pokhilenko et al., 1991). Garnets from these dunites relate to the lherzolite trend and Fe# is close to 0.1. The Fe#Ol (olivine equilibrated with chromites) of these chromites create a continuous trend decreasing together with pressures and joining with the garnet trend near 3 GPa. Ulvospinel component sharply grows in the lower part of the section, possibly due to reaction with protokimberlites. The inflection of the geothermal gradient is noted at the level of 5.5–6 GPa. The ilmenite P-Fe# trend also reveals a continuous increase upward in the interval from 7 to 4 GPa. Ilmenite-bearing metasomatites with comparatively low Fe# and increasing of Cr content in the ilmenites with decreasing pressure are found in the lower and upper parts of the mantle section.

5.2. Oxidation state in mantle beneath Kharamai field and Prianabarie

Oxidizing conditions were estimated using analyses of garnets using the monomineral version of Gudmundsson and Wood (1995), clinopyroxenes according to the published equation (Ashchepkov et al., 2012) (modified here) and chromites and ilmenites in monomineral variations of Chr-Ol and Ilm-Ol oxybarometers (Taylor et al., 1998). Peridotite (Cpx, Gar, Sp) minerals reveal close conditions in the P-$f(O_2)$ diagrams for each pipe from the Kharamai field and in the combined diagram. The widest variations were detected in the upper part of the mantle section. Presence of pyroxene-rich layer within 2.5–4.5 GPa interval is accompanied by the highest $f(O_2)$ fluctuation. In the lower unit the oxidation trend has an inflection near 5 GPa. Ilmenite $f(O_2)$ estimates (Taylor et al., 1998, monomineral version) reveal two branches divided at near 4.5 GPa. Untypical for magmatic systems, a decrease of $f(O_2)$ near this level is accompanied by increasing Cr. This possibly reflects reduction of the proto-kimberlitic melts due to interactions or assimilation of peridotite. Common increase of Cr content in Ilm to the upper part of SCLM is due to the

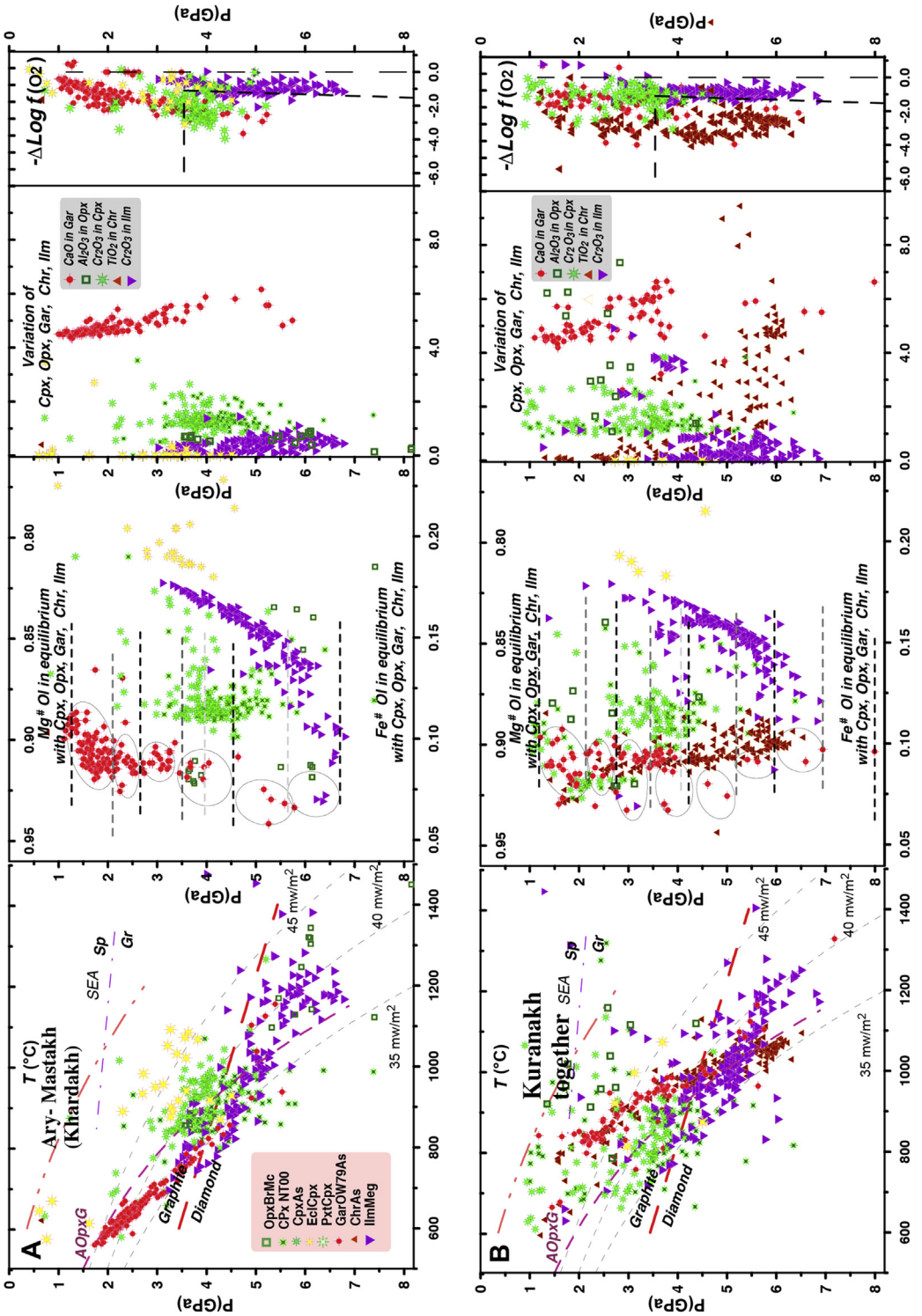

Figure 13. PTX$f(O_2)$ diagram for the minerals from the concentrates of the kimberlite pipes from (A) Khardakh pipe from Ary-Mastakh field, and (B) Kuranakh field pipes. Signs are as in Fig. 12.

continuous dissolution of SCLM substrate by proto-kimberlitic melts during ascent and creation of feeder vein system.

In the lower part, the garnet-bearing rocks mark three levels and two major ones coincide with those found for chromites. Ilmenites detect more oxidizing conditions in the lower part but in the middle pressure interval the highest of oxidation degrees of Gar, Cr and Cpx coincides with those found for ilmenites.

Two intervals of increasing upward oxidation state trends inflected near 3.5–4 GPa were observed in the upper part of SCLM beneath the Khardakh pipe (Ary-Mastakh field). The middle part of the section in the pyroxenite lens reveals the most diverse oxygen condition (Fig. 13A). Pyroxenes (Cr-diopsides, pyroxenitic augites and rare omphacite) in association with ilmenites are more highly oxidized, while the others demonstrate conditions close to those

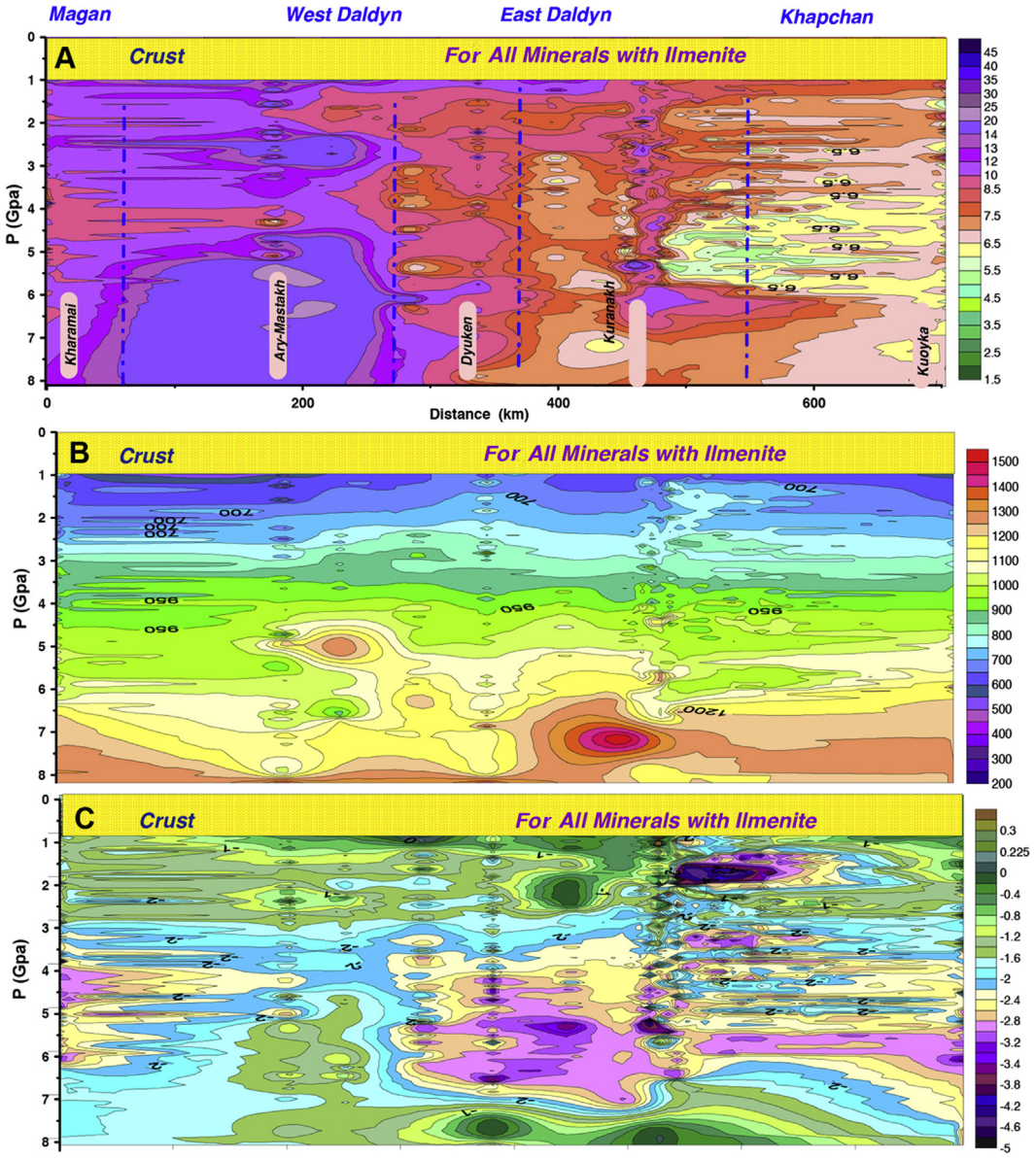

Figure 14. The SCLM profile using the Fe# and thermobarometry of xenocryst from Kharamai to Kuranakh filed. (A) *P* (GPa) - Fe# for all minerals, (B) *P* (GPa) - *T* (°C), (C) *P* (GPa) - $f(O_2)$ for all minerals.

determined from garnets. In the lower part of SCLM ilmenites demonstrate a stepped P-$f(O_2)$ trend which may correspond to differentiation in the small vein bodies distributed within several pressure intervals.

In the SCLM beneath the Kuranakh field the double P-$f(O_2)$ stepped trends extend through the whole mantle section from the SCLM base to the Moho. Trends for chromites and rare garnets $<-2\Delta$QMF are divided into 5 pressure intervals. Double lower arrays are located within the diamond stability field (McCammon et al., 2001). Chromites in the middle part of the SCLM are slightly more oxidized. They show and close in oxidation state, garnets show three separate in pressure intervals with the general $f(O_2)$ increase to the top of mantle section. The trend of the higher oxidation state -1 ± 1 ΔQMF for the ilmenites of pyroxene and rare garnets apparently corresponds to the system of veins and metasomatites, which should be created under the influence of the protokimberlitic melts. The highest oxidation state is found for the Cr-diopsides and ilmenites at 3–4 GPa pressure interval. The omphacites give more reduced conditions.

5.3. SW–NE transect through mantle beneath Kharamai field and Prianabarieto Kuoyka field

The SW to NE transect from Kharamai through Anabar fields to the Kuoyka field, also having early Triassic kimberlites like Djanga, was obtained using Surfer 8 software similar to the procedure used for the Arkhangelsk kimberlite region and central part of Siberia (Afanasiev et al., 2013; Ashchepkov et al., 2014). It is somewhat similar to the mantle profile compiled for Siberia and other kimberlite provinces by Griffin et al. (1999a). We used Fe# values for all minerals together with ilmenites marking magmatic systems and metasomatites (Fig. 14A), and also the profiles using

Please cite this article in press as: Ashchepkov, I.V., et al., Comparison of mantle lithosphere beneath early Triassic kimberlite fields in Siberian craton reconstructed from deep-seated xenocrysts, Geoscience Frontiers (2015), http://dx.doi.org/10.1016/j.gsf.2015.06.004

calculated temperature (Fig. 14B) and oxygen fugacity values (Fig. 14C). The separate pipes or groups of kimberlite pipes are used as a drill holes into the mantle. The horizontal scale is 700 km whereas the vertical scale in 270 km. Calculated Fe#Ol values for all the minerals were approximated by the kriging gridding method. The color contour maps show the isopotential lines of Fe#Ol for all minerals together.

The profile shows beneath the Anabar shield two lenses of rocks with increased Fe# (0.10–0.12) separated at 3.5 GPa into parts. The lenses refer to the Fe-rich dunites which may be typical for the Archean arc mantle (Gornova et al., 2013). The melt feeders and accompanied Ilm metasomatites (0.12–0.14 Fe#) are most frequent in the Ary-Mastakh which is supported by the presence of the large amount of microxenoliths of glimmerites and Phl-Ilm dunites in the kimberlites from these fields.

The Kharamai field shows a division into three large layers with the higher Fe# values near 3.5–4 GPa in pyroxenite lens and at 6 GPa corresponding to a heated layer or lithosphere-asthenosphere boundary. In the west part the SCLM beneath the Ary-Mastakh and Kuranakh the P-Fe# trends for garnets show different inclinations. The layering beneath the Khardakh pipe has more contrast and show more depletion in the lower part of SCLM.

6. Discussion

6.1. Structure of mantle sections and tectonic implications

Previous works (Ashchepkov et al., 2001, 2013a,b) determined that Siberian and other cratons reveal individual features of the structure of mantle sections in different terranes. The layering is more expressed in the fluctuations of the P-Fe# trends for the garnets (Ashchepkov et al., 2013a). The major dividing horizons determine the position of magma chambers, traced by megacrysts of ilmenites. The structural individual features are emphasized by the position of eclogite lenses and pyroxenite layers as well as PT estimates for different bodies possibly belonging to the some melt conduits and accompanied metasomatites. The veined peridotite groups and metasomatites mainly represent the dispersed clouds in the PT and P-Fe# diagrams (Figs. 12 and 13). The continuous trends with some clots for chromites possibly reflect the position of the large dunite veins and podiform chromite bodies similar to those found in ophiolites (Arai et al., 2004). They should mark the hydrous melts fluid migration. While the pyroxene refertilization trends and arrays correspond to the carbonatite and protokimberlite reaction associations and metasomatites.

According to accepted tectonic divisions the Kharamai field relates to the Magan terrane (Gladkochub et al., 2006; Rosen et al., 2006; Smelov and Zaitsev, 2013). The reconstructed mantle sections for pipe Mir, Internatsionalnaya pipes (Ashchepkov et al., 2010) and other large pipes in these terranes give sharply stepped P-Fe# garnet arrays according to distribution of the sub-calcic garnets and the clots of the ilmenite PT trends in the northern part of the Malo-Botuobinsky field. The mantle section beneath the Internatsionalnaya pipe according to the P-Fe# garnet trend may be also fertile and contain abundant pyroxenites and eclogites. At the same time, the structure of the mantle section under the Kharamai lithosphere block consists of 6 large units which do not reveal rhythmical contrasting stratification based on the garnet estimates. Such types of sections are more typical of the Daldyn and Markha terrane. But in the Daldyn terrane the sharp division into 6 separate structural units (Ashchepkov et al., 2010, 2013a) is characteristic. Three levels of stratigraphic divisions between these units in the lower part of the SCLM, possibly represent the paleoslabs or their groups (Pearson et al., 1995) and should control the position of magma chambers. Such types of layering with the three levels of ilmenite concentration in the lower SCLM, as in the SCLM beneath the Malysh and Tuzik pipes, was determined for the Zarnitsa mantle section. But the combined diagram for the SCLM beneath Kharamai shows the presence of two large ilmenite clouds. This is similar to the SCLM beneath the Internatsionalnaya pipe or Sytykanskaya pipe in the Alakit field.

The structure of the Ary-Mastakh field located at the boundary between the Magan and Daldyn terranes has no direct analogies in the Magan terrane. The location of the permeable zone is a possible reason of the high concentration of ilmenites and phlogopites and many pipes from this field. Maybe it is somewhat similar to the SCLM beneath the Mir pipe which shows a relatively fertile upper part and sharply exhausted lower part and a thick pyroxenite-eclogite lens. But the layering shows more contrast in the Malo-Botuobinsky field. Some pipes in the Kuoyka field such as Obnazhennaya (Taylor et al., 2003; Ashchepkov et al., 2010, 2013a,c; Howarth et al., 2014), which has also very depleted lower SCLM part and thick pyroxenite layer, reveal a very similar SCLM structure but belong to the Khapchan terrane.

The Kuranakh field has some similarities with the pipes from the Daldyn terrane where two large kimberlite fields are known. The SCLM beneath the Udachnaya pipe is separated into 6 sharply contrasting units (Ashchepkov et al., 2013b) and ilmenite PT estimates are mainly located in the lower part. One can also find rather thin layering to 12 units for the Kuranakh field SCLM. The thick pyroxenite-eclogite layer also exists. But the garnet trends and pyroxene compositions are quite different from those found in kimberlites from the northern Daldyn terrane. The high degree of depletion is typical for the mantle peridotites from SCLM beneath the Yubileinaya pipe and small pipes in this cluster.

6.2. Compositional features of the mantle sequences in different terranes

In all SCLM sections beneath kimberlites in the Anabar shield, we find an important enrichment by pyroxenite material of the upper parts of mantle lithosphere and amphibole metasomatism. Commonly it occurs in the peripheral parts of cratons like in the Kasai craton in Africa (Franz et al., 1996). But the lower part is sharply exhausted to dunites metasomatized to different degrees (Ashchepkov et al., 2001). The highly depleted mantle in the lower part is common for some parts of Kuoyka and other northern kimberlitic fields belonging to the Khapchan terrane. It seems that exhausting of the deeper horizons of the SCLM is not a characteristic feature of the marginal part of cratons, but is typical for the shield areas such as Aldan, northern part of Zimbabwe craton (Smith et al., 2009) and Greenland (Wittig et al., 2008).

The rarity or lack of sub-calcic garnets seems to be also rather common for the northern and eastern parts of the Siberian craton. For example, in the eastern part of craton in the Manchary field, such garnets have not been found yet in the lower part of mantle section (Smelov et al., 2010).

Presence of amphiboles of Cr-hornblende or pargasite type provides evidence about metasomatic modification of the upper part of the mantle sections in the 3.5–1.0 GPa interval of the Kharamai, whole Anabar and Prianabarie and Kuoyka fields. They are rather rare in the central part of the Siberian craton. In the center section of the Siberian craton, amphiboles of the richterite-type prevail (Ashchepkov et al., 2004).

The thick pyroxenite layer in the middle part of the SCLM beneath the Kharamai field (Fig. 12) and its heterogeneous heating is typical also for several regions of the Anabar shield and Kuoyka in

Please cite this article in press as: Ashchepkov, I.V., et al., Comparison of mantle lithosphere beneath early Triassic kimberlite fields in Siberian craton reconstructed from deep-seated xenocrysts, Geoscience Frontiers (2015), http://dx.doi.org/10.1016/j.gsf.2015.06.004

Prianabarie. The pyroxenite lens beneath Kharamai is located within 3–3.5 GPa interval. Commonly in the central part of craton it is found deeper. Thick pyroxenite lens (Pokhilenko et al., 1991; Ashchepkov et al., 2010) are characteristic for the Daldyn and Magan terranes at the level of ~4 GPa, but it is not typical for the Markha terrane.

Compared to the Mesozoic kimberlites, the late Devonian kimberlites contain higher amount of sub-calcic garnets. Even in the northern fields like the Toluopka or Orto-Yargin field located 450 km northward from the Kuranakh field (Babushkina, in press), the amount of such garnets is significant in the pipes and in placers.

The question is: what is the reason for the similarity of the SCLM in northern Siberia around Anabar shield, represented by the general depletion in the lower SCLM part and high degree of metasomatism in the upper part? Is it an original feature or was it created during the further history including the modification by possible subduction-related fluids or superplume events? It is possible also that the tectonic division within the crust does not coincide with the mantle structure.

The xenoliths which refer to depths of ~5–6 GPa (Ashchepkov et al., 2001; Griffin et al., 2005) have essentially dunitic compositions with porphyroclastic structure and the nests of garnets and pyroxenes which correspond to the refertilization type. Many dunites also contain phlogopites probably created in the permeable fracture zones such as transform faults or ancient sutures. Some dunites reveal porphyroclastic structures with recrystallization of olivine margins to fine grained aggregates. All these features seem to be of secondary origin.

It is possible that the position of heating corresponds to the olivine dislocation creep produced by hydrous fluids or melts are located just near ~6.0–6.5 GPa (Karato, 2010; Peslier et al., 2010), which mainly determines the lithosphere–Asthenosphere Boundary (LAB) position beneath the cratons in Phanerozoic time.

Some PT estimates corresponding to 7.0 GPa and lower, and the presence of Cr-rich garnets in the Kharamai kimberlites probably means that there are the relics of thick lithosphere beneath the Kharamai field and some regions in the Anabar shield.

The diverse models of lithospheric keel formation (Lee et al., 2011) suggest presence of the olivine-rich layers in lithospheric mantle keel making it more buoyant than fertile convecting mantle (Artemieva, 2009). Thick dunitic cores could produce upwelling corresponding to the shields within cratons, especially if they have deep roots because depths >8 GPa are at the boundary of Ol-melt density inversion (Agee et al., 1982).

The P-Fe$^{\#}$Ol trend from 0.7 in the SCLM base to 0.11–0.12 in the top of the Kharamai peridotite mantle column is not typical for Archean mantle sequences. The upper enrichment may be attribute to plume influence because basaltic melts are mainly reacting with the upper part of the mantle column in 3–1.5 GPa, within the depression of the H_2O-bearing melts (Tappe et al., 2007). The origin of dunites which are common in the Anabar mantle may be a high degree melting of Archean mantle diapirs. But some dunites with the Gar-Opx-Cpx nests from Anabar and surroundings have rather high Fe$^{\#}$Ol ~0.085–0.1 (Ashchepkov et al., 2001) which is not typical for the Archean mantle (Griffin et al., 2003), and possibly relate to the refertilized associations. Slightly elevated Fe$^{\#}$Ol is an attribute of ancient arc peridotites (Gornova et al., 2013). But most peridotites have the range of Fe$^{\#}$Ol calculated for garnets ~0.5 to 0.7 (Ashchepkov et al., 2013a) which is close to Archean peridotites having Fe$^{\#}$ close to 0.067 (Gornova et al., 2013). Modern fore arc-mantle peridotite close to the Mariana type (Ohara et al., 2002) olivines have higher Fe$^{\#}$ values 0.07–0.08. Ancient Sp peridotites from the Premier pipe in South Africa reveal also rather elevated Fe$^{\#}$Ol (0.09–0.08) (Grégoire et al., 2005).

6.3. Geochemistry of minerals and parental melts as the signs of the geodynamic environment and its evolution

Geochemical signs of garnets from the mantle peridotites of the Kharamai field with a large quantity of humped REE patterns (Fig. 7A, Gr1-2) were not detected before in peridotitic associations from the Magan block (Griffin et al., 2005), and mostly refer to the pyroxenite layer. Another large amount of garnet (Fig. 7A, Gr3) relates to the lower part of SCLM. They reveal the spectra of high $(La/Yb)_n$ ratios and M-HREE depressions typical of garnet harzburgites (Ionov et al., 2010). One analysis shows rather high HFSE concentrations. Reconstructions with the KD (Hauri et al., 1994) of the parental melts for the garnets show three different patterns. The convex upward patterns commonly are attributed to some types of clinopyroxenes (Gr1) (Fig. 15). In other words the melts produced such garnets were dissolved essential amount of the clinopyroxenes. The concave downward patterns are typical for enstatites of harzburgite type (Gr3). Such type of dissolution could take place after the addition of hydrous melts which extends the garnet stability field. To obtain the melt which created clinopyroxenes, the calculated melt compositions parental for the garnets were divided by the partition coefficients of Cpx/melt after Hart and Dunn (1993). But for the exact determination of primary clinopyroxenes composition it is necessary to know the composition of the melts which dissolved the garnets which should be subtracted from the reconstructed melts.

Note that melts which are contaminated by the significant amount of dissolved orthopyroxenes of the island arc type having large MHEE depressions and elevated LREE (Ionov et al., 2013), should crystallize garnets with the patterns with M-HEE depressions common for some diamond associations (Stachel and Harris, 2008).

The analyses of garnets of Gr2-3 after a second inversion (Supplement 3, Fig. 1C) show linear spectra in LMREE and elevation in the HREE branch. Obtained concave downward from Gd to Tb REE spectra (Gr1) show some similarities with some boninite island arc melts (Smithies, 2002; Almeev et al., 2013), and those with flatter HREE are close to clinopyroxenes from granular Udachnaya peridotites (Ionov et al., 2010; Ashchepkov et al., 2013b).

Melts calculated for the Gr3 show patterns closest to garnet harzburgites from ancient ophiolitic complexes (Gornova et al., 2013). The spider diagrams show similarity in the left part of the diagrams with the continuous rise of incompatible components and peaks in U, Pb elevated LILE and small depression in Y. Anomalies in U, Th and Ta may be a sign of carbonatitic melts (Andrade et al., 2008). The possible hypothesis is deep seated melting in the arc setting with participation of some sediments (Condie et al., 2001) or metasomatized by arc melts (Hastie et al., 2011). Such a question cannot be solved without isotopy of clinopyroxene xenocrysts.

The high LREE of the orthopyroxenes suggests the high participations of fluids and Y anomalies may be attributed to the highly depleted peridotite source. Such melts may possibly not be of subduction-related type because they have no Eu anomalies. The melts parental for clinopyroxenes with highly inclined straight line REE patterns may be regarded as low degree partial melts in the garnet stability field having carbonatitic signatures, because they have elevation in U, Th and Sr peaks and small troughs in some HFSE such as Hf, Nb.

For the melts which produced mantle pyroxenes of the Kharamai field (Fig. 15B), the degree of melting must be ~0.05–0.1%, and the Gar/Cpx ratio of the parental rocks should be rather high

Please cite this article in press as: Ashchepkov, I.V., et al., Comparison of mantle lithosphere beneath early Triassic kimberlite fields in Siberian craton reconstructed from deep-seated xenocrysts, Geoscience Frontiers (2015), http://dx.doi.org/10.1016/j.gsf.2015.06.004

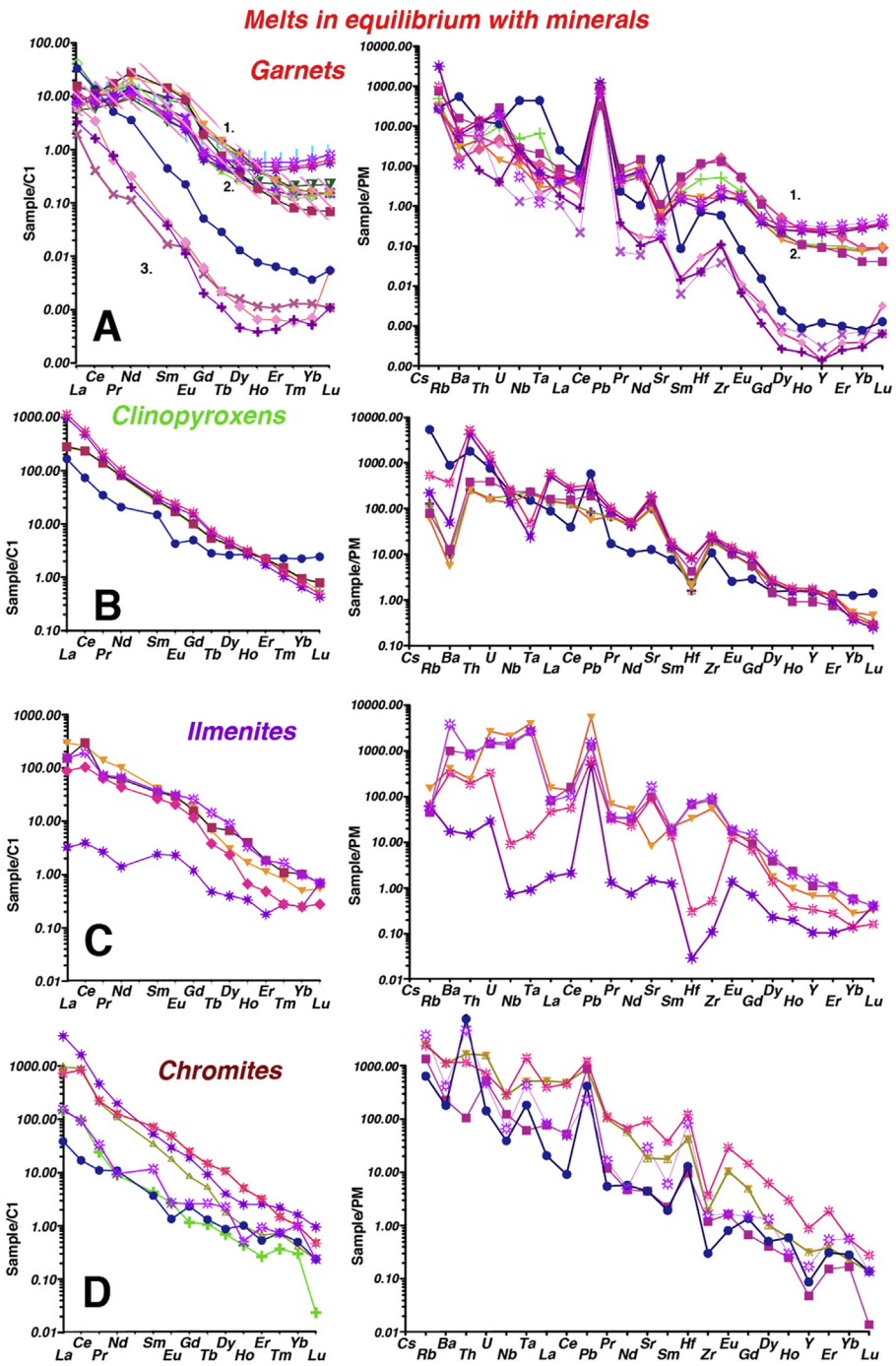

Figure 15. REE patterns and TRE spider diagrams for the melts in equilibrium with the minerals from deep seated xenocrysts from the kimberlite pipes Kharamai field. The TRE compositions of parental melt for Cpx are reconstructed with KD after Hart and Dunn (1993), for garnets after Hauri et al. (1994).

(1–2) (Fig. 2, Supplement 3) which corresponds to harzburgites, because lherzolitic clinopyroxenes should have asymmetric bell-like patterns (Ashchepkov et al., 2011). Such characteristics of the studied regions are also shown by some mantle clinopyroxenes from the Alakit field (Ashchepkov et al., 2004). Elevated Th and U concentrations suggest that parental melts may be carbonatitic (Nelson et al., 1988). The melt parental for the omphacite reveals signatures of primitive Mg-andesites with the Eu peaks (Jolly et al., 2007), but they are not close to adakites (Eyuboglu et al., 2011) having commonly Ta-Nb minima.

Parental melts for ilmenite reconstructed with KD (Zack and Brumm, 1998) (Supplement 3, Fig. 2A) show signatures regarded to be carbonatitic. They have inclined patterns with inflections in MREE and other part of patterns which may be a result of the tetrad effect. There are small peaks in Ce. HFSE varies from elevated to depleted, possibly in accordance with oxidation state. The peaks in Pb suggest that these melts were not differentiated and were created as partial melts.

The REE patterns of the melts which produced chromites found with KD (Klemme et al., 2009; Supplement 3, Fig. 2B) are even more

Please cite this article in press as: Ashchepkov, I.V., et al., Comparison of mantle lithosphere beneath early Triassic kimberlite fields in Siberian craton reconstructed from deep-seated xenocrysts, Geoscience Frontiers (2015), http://dx.doi.org/10.1016/j.gsf.2015.06.004

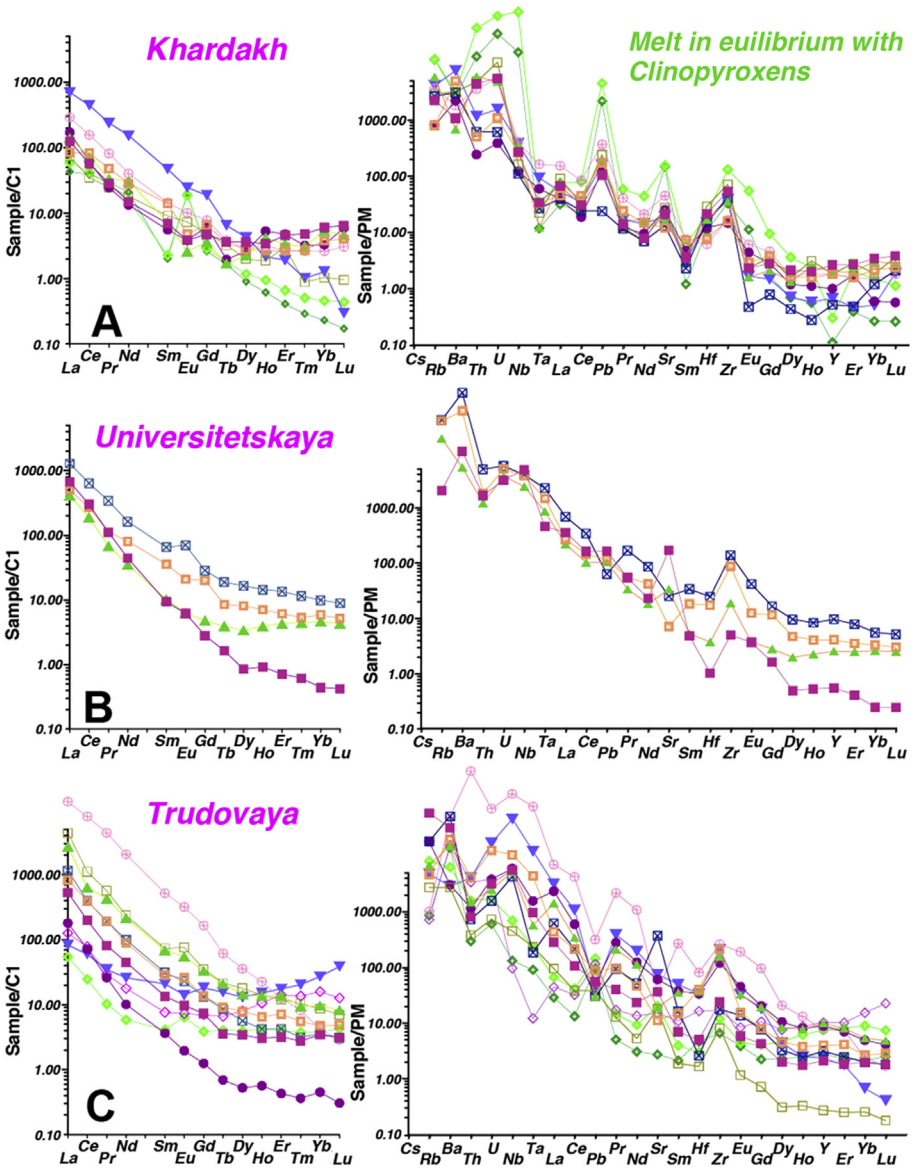

Figure 16. REE patterns and TRE spidergrams for the melts in equilibrium with the clinopyroxenes from deep seated xenocrysts from the kimberlite pipes Khardakh pipe (A) Ary-Mastakh field, (B) Universitetskaya pipe and (C) Trudovaya pipe of Kuranakh field.

inclined than all the others, which suggests that they were low degree partial melts of peridotites where garnet content was rather high, because the Gar/Cpx ratio in general regulates the inclination. Peaks in Pb, Ta, Pb may result from the involvement in melting of the impurities on grain surfaces (Bedini and Bodinier, 1999), and decoupling of Ta, Nb, Zr and Hf probably suggests rutile contribution (Foley et al., 2000).

Melts parental for clinopyroxenes from the Khardakh pipe in Ary-Mastakh field (Fig. 16A) show two modes of TRE patterns. Though LREE levels near 100/PM and flatter HREE parts are close to primitive andesites (Jolly et al., 2007) showing continuous growth of incompatible elements and without fractionation of HFSE, the elevated Zr-Hf and peaks of Sr, Pb probably implies their origin from low degree partial melts with intergranular space material (Bedini and Bodinier, 1999). The straight line REE patterns with different REE levels reveal high peaks of Th, U, and Ba. All these features may mean some participation of subduction-related fluids.

Geochemistry of pyroxenes from the peridotites of SCLM beneath the Kuranakh field (Fig. 16B, C) is also not typical for the central section of the Siberian craton (Nimis et al., 2009; Ionov et al., 2010; Ashchepkov et al., 2013a). Melts parental for the pyroxene from the Universitetskaya pipe with low $(La/Yb)_n$ (Fig. 16B) ratios are from the garnet-spinel mantle facies showing slightly U-shaped patterns with elevated LREE assumed to be participation of a high amount of fluid. One composition with high REE inclination shows enrichment in Nb, Ta, Th, U and Zr, probably reflecting ilmenite dissolution.

Similar TRE patterns are shown by most clinopyroxene parental melts from the Trudovaya pipe (Fig. 16C). The clinopyroxene's features from the Universitetskaya pipe (Fig. 16B) and Trudovaya from the Kuranakh field as well as Khardakh pyroxene from the Ary-Mastakh field also show the participation of fluids. Variations in HREE suggest different fractions of garnet in parental rocks.

Garnets from the upper part of the section, along with pyroxene, probably demonstrate the participation of crustal material or

Please cite this article in press as: Ashchepkov, I.V., et al., Comparison of mantle lithosphere beneath early Triassic kimberlite fields in Siberian craton reconstructed from deep-seated xenocrysts, Geoscience Frontiers (2015), http://dx.doi.org/10.1016/j.gsf.2015.06.004

tonalite melt signatures and their hybridization with mantle peridotites.

Hence, clinopyroxenes from the Anabar region reveal the similarities of geochemistry with clinopyroxenes from arc-type ophiolite rocks. The high LREE content and concave downward patterns suggest absence of garnets in the source and high influence of the fluids, which may be an attributed to an arc origin. However, most calculated using division to Cpx KD melts have no HFSE depletions which are common for melts with H_2O-bearing fluids. This probably means the reducing conditions of the ancient mantle. But even high dense fluid found in diamonds (Tomlinson and Müller, 2009) reveals such anomalies.

We tried to model some cases of melting taking the composition of harzburgite with the nearly flat TRE pattern without deep HFSE anomalies (Ionov et al., 2010) as the starting peridotite composition. We use two models: (1) of melting with different melting degree (F) and (2) fusion with various Gar-Cpx (Supplement 3, Fig. 3A, B) ratios and the same F. Both of them suggest very low melting degree which could take part only in presence of fluid. Modeling with the additional fractionation of the garnets and mixing with the dense fluids (Supplement 3, Fig. 3C) (Tomlinson and Müller, 2009) shows possibility of such processes. But they could proceed only in highly reduced conditions without precipitation of oxides making HFSE anomalies.

There is no essential difference in the geochemistry of clinopyroxenes from Anabar shield from Khardakh pipe (Ary-Mastakh field), Universitetskaya (Kuranakh fields) referring to the Daldyn and Khapchan terranes respectively. Reconstructions of the ancient melts that created clinopyroxenes give highly LREE-rich and inclined concave downward patterns without strong anomalies except for small Zr peaks. Such geochemical features have no analogies in modern mantle melts.

6.4. Possible model of Siberian continent growth

The principle feature of the mantle sections in the northern part of the Siberian craton are: rather simple division without sharp layering, the thick pyroxenite layer and a high degree of metasomatism in the upper SCLM. Abundance of Na-amphiboles, eclogites and pyroxenitic assemblages with the enriched LREE and incompatible elements also reflect the environment close to marginal continental signatures. This is supported also by the geochemistry of the xenocryst minerals and their parental melts (Figs. 15 and 16).

The geochemical features of the minerals such as TTG TRE signatures of garnets in the Ary-Mastakh show possible arc settings. And all studied kimberlite fields including Kuranakh and Kuoyka in Birekte terrane possibly are close to the environment of marginal micro continents similar to those constituting Indonesia. They also have very enriched upper parts of the mantle section and depleted lower parts below 4 GPa (Nixon and Boyd, 1979).

An abundance of eclogitic pyroxenes and garnets in concentrates show an arc environment of mantle sequences in Prianabarie and northern Yakutia. High variation of the $Fe^{\#}$ in the lower part suggests that the mantle column was constructed from heterogeneous units and possibly subjected to interaction with melts/fluids. Laterally the SCLM structures are not homogeneous and formed from several blocks which were accreted together in the Anabar collision system ~1.8–1.6 Ga (Rosen et al., 2007).

These PT reconstructions for xenocrysts of the Kharamai kimberlite with definite layered structure of SCLM consist of 5 or more likely 7–8 levels. The P-$Fe^{\#}$ upward trends are not common for SCLM in Devonian time (Ashchepkov et al., 2013a).

Earlier a model of low angle subduction on top of the mantle plumes was suggested to explain the similarity of the mantle layering consisting from 10 to 12 separate layers in the central part of Yakutia (Ashchepkov et al., 2010, 2013a). The alternative hypothesis of the mantle keel is merging of the stacked slab at the margin of the continents (Griffin and O'Reilly, 2007), and is also a possible mechanism of lithosphere growth beneath the Anabar Shield.

The transect from the Magan to Khapchan terranes and further to the Birekte terrane shows the difference in the structure of these units. It supports also a rather unusual feature of the Anabar shield SCLM, composed from rather Fe-rich but depleted in modal composition peridotites (Fig. 14).

To explain the origin of pyroxenite–eclogite layering we suggest that it was formed in the early Archean when the geothermal gradient was higher and eclogites could not cross the 130 km boundary (Gerya, 2014) and were partly remelted. Another possible mechanism is loading of the Mg-rich cumulates derived from the TTG in the base of arc magmatic systems (Horodyskyj et al., 2007).

It is possible to propose a combined model that accounts for possible variants (Fig. 17).

6.5. Interaction of the superplume with the mantle lithosphere

The Permo-Triassic plume magmatism appeared several hundred kilometers to the north-west in the Meimecha Province (Arndt et al., 1995; Kogarko and Ryabchikov, 2000). All mantle sections sampled by lower Triassic kimberlites reveal significant heating in the lower part of the mantle column within the 5–6 GPa interval or upper at 5 GPa and depletion to dunites with rare garnets. While the Devonian superplume stage is

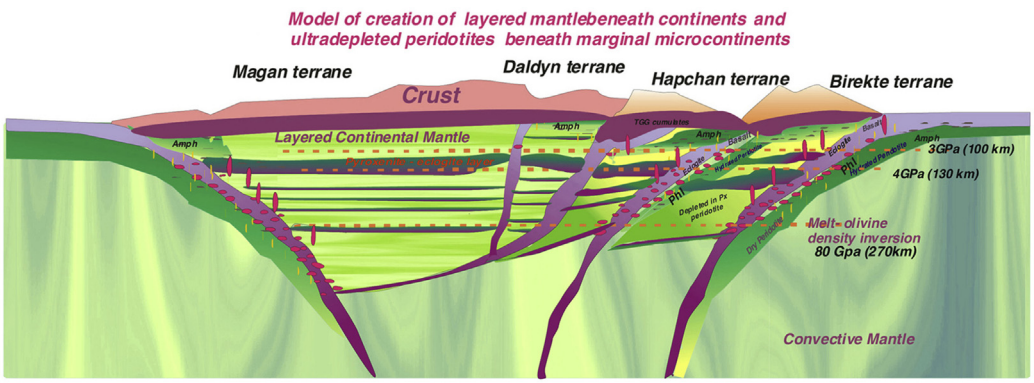

Figure 17. Model of the creation of mantle beneath Kharamai and Anabar kimberlite fields.

Please cite this article in press as: Ashchepkov, I.V., et al., Comparison of mantle lithosphere beneath early Triassic kimberlite fields in Siberian craton reconstructed from deep-seated xenocrysts, Geoscience Frontiers (2015), http://dx.doi.org/10.1016/j.gsf.2015.06.004

characterized by the presence of sheared peridotites (Ionov et al., 2010) and refertilization (Howarth et al., 2014). The formation of garnet dunites (Pokhilenko et al., 1991) probably took part in the early stages of craton creation. Thick pyroxenite lens is also typical, as in Aldan, Chompolo (Ashchepkov et al., 2001, 2010) or 4 GPa (Obnazhennaya, Kuoyka field) (Taylor et al., 2003; Ashchepkov et al., 2014). They also reveal the distinct Mesozoic linear pyrope pyroxenite trends started from different Cr contents and reflect continuous reaction of the plume-related melts with the peridotites (Howarth et al., 2014). The beginning of the linear Cr-Ca trend produced by the essentially carbonatite magma (Pokhilenko et al., 2015) is determined by the depth of plume melt intrusions.

Could interaction with the plume also be the reason for the depletion of the lower SCLM part and pyroxenization and metasomatism in the upper part? The depletion of lherzolites-harzburgites to dunites (10–20% of melting) from the base (250 km) to 100 km should be a great event which could produce enough melt to form the 10–20 km pyroxenite layer which may have crystallized in the middle part of SCLM or reacted with the eclogites producing hybrid melts and pyroxenites as was suggested for Obnazhennaya (Taylor et al., 2003). Prevalence of pyroxenites may be the attribute of separate pipes tracing local zones. Even in the Kuoyka field, large amounts of pyroxenites are not common for each pipe (Ashchepkov et al., 2013a,b,c,d). Geochemical exploration evidence mainly informs about the refertilization processes (Taylor et al., 2003; Howarth et al., 2014) accompanying the plume influence, and without detailed isotopic geochemical data, it is not possible to decipher the origin of dunites. Presence of the pyroxenite layers in many SCLM sections worldwide in other cratons suggest that these layers are of primary origin in early Archean time.

Exhaustion in the lower part of the studied sections to dunites and generation of basalts could possibly be connected with the influence of superplume. However, in the Anabar region and nearby regions, basaltic magmatism did not appear. The $Fe^{\#}Ol$ increase within 3.5–1 GPa (Ashchepkov et al., 2013a) could be explained as a result of the plume melts differentiation and interaction during ascend. They could produce enriched lherzolites and pyroxenites with Fe-rich and high-Al pyroxenes. And P-$Fe^{\#}$ upward trend due to differentiation of the host melts during ascent which is determined also in the mantle section of the Khardakh pipe (Ashchepkov et al., 2013a). But there are no geochemical signs of interaction with the plume melt in the geochemistry of pyroxenes and garnets. Usually pyroxenes and garnets produced by plume-related melts have smooth round spidergrams (McDonough and Sun, 1995) which is not found for mantle xenocrysts of the Kharamai field. The rarity or absence of the typical sheared peridotites is also distinct feature of SCLM sections sampled by the early Triassic kimberlites.

The single diamondiferous pipe of early Triassic age is Malokuonamskaya in the Karanakh field containing abundant eclogitic garnets, but peridotitic garnets with dunitic affinity are rare, which is possibly a specific feature of the Anabar region which is different from central Siberia South Africa, Canada and other kimberlitic provinces worldwide (Stachel and Harris, 2008; Cartigny et al., 2009).

The considerable decrease of the thickness and delamination of the lithospheric keel, which was assumed (Griffin et al., 1999a,b, 2005) on the basis of previous versions of garnet thermobarometry (Ryan et al., 1996) was not found, but it is slightly reduced to 190–220 km (5.5–6.5 GPa) judging by geophysical data (McKenzie and Priestley, 2008). Similar processes took place beneath the Colorado plateau (Coopersmith et al., 2003). In the central regions of the Siberian craton the thickness usually corresponds to 250–270 km (7–8 GPa). For Kharamai and Anabar the elevated geothermal gradients in the middle and upper parts of the SCLM sections are more notable than for the mantle section found beneath the Udachnaya pipe (Ashchepkov et al., 2013b) and some other large Devonian kimberlites pipes of the Siberian craton (Ashchepkov et al., 2010, 2013a). These phenomena may be associated with the influence of the Devonian superplume responsible for mantle heating. These phenomena may be associated with the influence of the Devonian superplume responsible for mantle heating. These phenomena may be associated with the influence of the Devonian superplume responsible for mantle heating.

7. Conclusions

(1) Structure of the mantle section of the Kharamai field essentially differs from studied sections of the mantle lithosphere in Magan (Malo-Botuobinskoe filed) and other terranes of the Siberian craton and mantle sections of the Anabar shield show individual features of SCLM beneath each kimberlite field.
(2) Geochemistry of pyroxene garnets and ilmenites of the Kharamai field differ from the chemical features of mantle minerals from the Anabar shield. Parental melts for the minerals in SCLM beneath Anabar reveal increase of the incompatible components and LREE, suggesting high saturation in volatiles typical for (continental) island arc mantle.
(3) Abundance of the Na-Cr-amphibole and other signs of mantle metasomatism in the upper part of the mantle, and a rather thick pyroxenite eclogite layer 2.5–4 GPa interval is the sign of the marginal signature of the craton SCLM.
(4) There is no evidence for delamination of lithosphere in the northern part of Siberian craton. But the decrease of the mantle keel thickness from 250 to 220 km after the Permian–Triassic superplume is thought to be the result of heating and plume melt interaction with mantle peridotites and low diamond grade of early Triassic kimberlites.

Acknowledgments

Appreciation to the laboratories of Analytical Center IGM SD Russian Academy of Science. Many thanks to ALROSA Company and to S.I. Kostrovitsky for the given concentrates and Nick Roberts for useful comments. Research is supported by grants RFFI 11-05-00060a and 11-05-91060-PICS.

Appendix A. Supplementary data

Supplementary data related to this article can be found at http://dx.doi.org/10.1016/j.gsf.2015.06.004.

References

Afanasiev, V.P., Pokhilenko, N.P., Lobanov, S.S., 2011. Placer diamond potential of the Siberian craton: possible sources and ages. Geology of Ore Deposits 53, 474–477.
Afanasiev, V.P., Ashchepkov, I.V., Verzhak, V.V., O' Brien, H., Palessky, S.V., 2013. PT conditions and trace element variations of picroilmenites and pyropes from the Arkhangelsk region. Journal of Asian Earth Sciences 70–71, 45–63.
Agee, J.J., Garrison, J.R., Taylor, L.A., 1982. Petrogenesis of oxide minerals in kimberlite, Elliott County, Kentucky. American Mineralogist 67, 2842.
Almeev, R.R., Kimura, J.-I., Ariskin, A.A., Ozerov, A.Yu, 2013. Decoding crystal fractionation in calc-alkaline magmas from the Bezymianny Volcano (Kamchatka, Russia) using mineral and bulk rock compositions. Journal of Volcanology and Geothermal Research 263, 141–171. http://dx.doi.org/10.1016/j.jvolgeores.2013.01.003.
Andrade, F.R.D.D., Moller, P., Dulski, P., 2008. Zr/Hf in carbonatites and alkaline rocks: new data and a re-evaluation. Brazilian Journal of Geology 32 (3), 361–370.

Arai, S., Uesugi, J., Ahmed, A.H., 2004. Upper crustal podiform chromitite from the northern Oman ophiolites the stratigraphically shallowest chromitite in ophioliteand its implication for Cr concentration. Contributions to Mineralogy and Petrology 147, 145–154.

Arndt, N., Lehnert, K., Vasil'ev, Y., 1995. Meimechites: highly magnesian lithosphere-contaminated alkaline magmas from deep subcontinental mantle. Lithos 34, 41–59.

Artemieva, I.M., 2009. The continental lithosphere: reconciling thermal, seismic, and petrologic data. Lithos 109, 23–46.

Ashchepkov, I.V., Vladykin, N.V., Saprykin, A.I., Khmelnikova, O.S., 2001. Composition and thermal structure of the mantle in peripheral parts of Siberian craton. Revista Brasileira de Geociencias 31, 527–536.

Ashchepkov, I.V., Vladykin, N.V., Nikolaeva, I.V., Palessky, S.V., Logvinova, A.M., Saprykin, A.I., Khmel'nikova, O.S., Anoshin, G.N., 2004. Mineralogy and geochemistry of mantle inclusions and mantle column structure of the Yubileinaya Kimberlite pipe, Alakit field, Yakutia. Doklady Earth Sciences 395, 517–523.

Ashchepkov, I.V., Logvinova, A.M., Pokhilenko, N.P., Kuligin, S.S., Malygina, E.V., Kostrovitsky, S.I., Khemelnikova, O.S., 2007. Developing of the Models of Structures of Mantle Columns beneath the Kimberlites Pipes for the Improving of the Prospecting of Diamond Deposits Using the Petrological and Geochemical Criteria for the Deep Seated Parageneses in Kimberlites. Report on IGM – ALROSA project 2-05. 355 p. v.1-2 (Supplements with analyses).

Ashchepkov, I.V., Pokhilenko, N.P., Vladykin, N.V., Logvinova, A.M., Kostrovitsky, S.I., Afanasiev, V.P., Pokhilenko, L.N., Kuligin, S.S., Malygina, L.V., Alymova, N.V., Khmelnikova, O.S., Palessky, S.V., Nikolaeva, I.V., Karpenko, M.A., Stagnitsky, Y.B., 2010. Structure and evolution of the lithospheric mantle beneath Siberian craton, thermobarometric study. Tectonophysics 485, 17–41.

Ashchepkov, I.V., André, L., Downes, H., Belyatsky, B.A., 2011. Pyroxenites and megacrysts from Vitim picrite-basalts (Russia): polybaric fractionation of rising melts in the mantle? Journal of Asian Earth Sciences 42, 14–37.

Ashchepkov, I.V., Rotman, A.Y., Somov, S.V., Afanasiev, V.P., Downes, H., Logvinova, A.M., Nossyko, S., Shimupi, J., Palessky, S.V., Khmelnikova, O.S., Vladykin, N.V., 2012. Composition and thermal structure of the lithospheric mantle beneath kimberlite pipes from the Catoca cluster, Angola. Tectonophysics 530–531, 128–151.

Ashchepkov, I.V., Vladykin, N.V., Ntaflos, T., Downes, H., Mitchel, R., Smelov, A.P., Rotman, A.Ya, Stegnitsky, Yu, Smarov, G.P., Makovchuk, I.V., Nigmatulina, E.N., Khmelnikova, O.S., 2013a. Regularities and mechanism of formation of the mantle lithosphere structure beneath the Siberian Craton in comparison with other cratons. Gondwana Research 23, 4–24.

Ashchepkov, I.V., Ntaflos, T., Kuligin, S.S., Malygina, E.V., Agashev, A.M., Logvinova, A.M., Mityukhin, S.I., Alymova, N.V., Vladykin, N.V., Palessky, S.V., Khmelnikova, O.S., 2013b. Deep-seated xenoliths from the Brown Breccia of the Udachnaya Pipe, Siberia. In: Pearson, D.G., et al. (Eds.), Proceedings of 10th International Kimberlite Conference, V1, Special Issue of the Journal of the Geological Society of India, pp. 59–74.

Ashchepkov, I., Kostrovitsky, S., Ovchinnikov, Y., Tychkov, N., Khmelnikova, O., Palessky, S., 2013c. New model of the mantle lithosphere beneath Kuoyka kimberlite field Yakutia. Geophysical Research Abstracts 15, EGU2013–14097.

Ashchepkov, I.V., Downes, H., Mitchell, R., Vladykin, N.V., Coopersmith, H., Palessky, S.V., 2013d. Wyoming craton mantle lithosphere: reconstructions based on Sloan and Kelsey Lake kimberlite xenocrysts. In: Proceedings of 10th International Kimberlite Conference. Special Issue of the Journal of the Geological Society of India, vol. 1, pp. 59–73.

Ashchepkov, I.V., Vladykin, N.N., Ntaflos, T., Kostrovitsky, S.I., Prokopiev, S.A., Downes, H., Smelov, A.P., Agashev, A.M., Logvinova, A.M., Kuligin, S.S., Tychkov, N.S., Salikhov, R.F., Stegnitsky, Yu. B., Alymova, N.V., Vavilova, M.A., Minin, V.A., Babushkina, S.A., Ovchinnikov, Yu. I., Karpenko, M.A., Tolstov, A.V., Shmarov, G.P., 2014. Layering of the lithospheric mantle beneath the Siberian Craton: modeling using thermobarometry of mantle xenolith and xenocrysts. Tectonophysics 634, 55–75. http://dx.doi.org/10.1016/j.tecto.2014.07.017.

Babushkina, S.A., 2014. Typomorphism of the garnets from Zapretnaya pipe. Otechestvennaya Geologia (in press).

Bedini, R.M., Bodinier, J.-L., 1999. Distribution of incompatible trace elements between the constituents of spinel peridotite xenoliths: ICPMS data from the East African Rift. Geochimica et Cosmochimica Acta 63, 3883–3990.

Bleeker, W., 2003. The late Archean record: a puzzle in ca. 35 pieces. Lithos 71, 99–134.

Brakhfogel, F.F., 1984. Geological Aspects of Kimberlite Magmatism in the North-Eastern Siberian Platform. Yakutian branch of SO AN USSR Press, Yakutsk, p. 128 (in Russian).

Brey, G.P., Kohler, T., 1990. Geothermobarometry in four-phase lherzolites II. New thermobarometers, and practical assessment of existing thermobarometers. Journal of Petrology 31, 1353–1378.

Cartigny, P., Farquhar, J., Thomassot, E., Harris, J.W., Wing, B., Masterson, A., McKeegan, K., Stachel, T., 2009. A mantle origin for Paleoarchean peridotitic diamonds from the Panda kimberlite, Slave Craton: evidence from ^{13}C-, ^{15}N- and $^{33,34}S$-stable isotope systematic. Lithos 112 (S2), 852–864.

Cherenkov, V.G., Komarov, A.N., Cherenkova, V.G., Ilupin, I.P., 1987. On kimberlite ages of the Kharamai field. Doklady Akademii Nauk SSSR 29, 195–199.

Condie, K.C., Wilk, M., Rosen, D.M., Zlobin, V.L., 2001. Geochemistry of metasediments from the Precambrian Hapschan Series, eastern Anabar Shield, Siberia. Precambrian Research 50, 37–47.

Coopersmith, H.G., Mitchell, R.H., Hausel, W.D., 2003. Kimberlites and Lamproites of Colorado and Wyoming, USA. Guidebook for the VIIIth International Kimberlite Conference, Colorado and Wyoming Field Trip, p. 32.

Dantas, C., Grégoire, M., Koester, E., Conceição, R.V., Rieck Jr., N., 2009. The lherzolite–websterite xenolith suite from Northern Patagonia (Argentina): evidence of mantle–melt reaction processes. Lithos 107, 107–120.

Eyuboglu, Y., Santosh, M., Chungc, S.-L., 2011. Crystal fractionation of adakitic magmas in the crust–mantle transition zone: petrology, geochemistry and U–Pb zircon chronology of the Seme adakites, eastern Pontides, NE Turkey. Lithos 121, 151–166.

Foley, S.F., Barth, M.G., Jenner, G.A., 2000. Rutile/melt partition coefficients for trace elements and an assessment of the influence of rutile on the trace element characteristics of subduction zone magmas. Geochimica et Cosmochimica Acta 64, 933–938.

Franz, L., Brey, G., Okrusch, M., 1996. Steady state geotherm, thermal disturbances and tectonic development of the lower lithosphere underneath the Gibeon Kimberlite Province, Namibia. Contributions to Mineralogy and Petrology 126, 181–198.

Fraser, D.G., Lawless, P.J., 1978. Palaeogeotherms – implications of disequilibrium in garnet lherzolite xenoliths. Nature 273, 220–222.

Gerya, T., 2014. Precambrian geodynamics: concepts and models. Gondwana Research 25, 442–463. http://dx.doi.org/10.1016/j.gr.2012.11.008.

Gladkochub, D.P., Pisarevsky, S.A., Donskaya, T.V., Natapov, L.M., Mazukabzov, A.M., Stanevich, A.M., Sklyarov, E.V., 2006. Kuranakh, in terms of Rodinia hypothesis. Episodes 29, 169–174.

Gornova, M.A., Belyaev, V.A., Belozerova, O.Yu, 2013. Textures and geochemistry of the Saramta peridotites (Siberian craton): melting and refertilization during early evolution of the continental lithospheric mantle. Journal of Asian Earth Sciences 62, 4–17.

Gregoire, M., Bell, D.R., Le Roex, A.P., 2003. Garnet lherzolites from the Kaapvaal Craton (South Africa): trace element evidence for a metasomatic history. Journal of Petrology 44, 629–657.

Grégoire, M., Tinguely, C., Bell, D.R., le Roex, A.P., 2005. Spinel lherzolite xenoliths from the Premier kimberlite (Kaapvaal craton, South Africa): nature and evolution of the shallow upper mantle beneath the Bushveld complex. Lithos 84, 185–205.

Griffin, W.L., O'Reilly, S.Y., 2007. Cratonic lithospheric mantle: is anything subducted? Episodes 30, 43–53.

Griffin, W.L., Ryan, C.G., Kaminsky, F.V., O'Reilly, S.Y., Natapov, L.M., Win, T.T., Kinny, P.D., Ilupin, I.P., 1999a. The Siberian lithosphere traverse: mantle terranes and the assembly of the Siberian Craton. Tectonophysics 310, 1–35.

Griffin, W.L., Shee, S.R., Ryan, C.G., Win, T.T., Wyatt, B.A., 1999b. Harzburgite to lherzolite and back again: metasomatic processes in ultramafic xenoliths from the Wesselton kimberlite, Kimberley, South Africa. Contributions to Mineralogy and Petrology 34, 232–250.

Griffin, W.L., Spetsius, Z.V., Pearson, N.J., O'Reilly, S.Y., 2002. In-situ Re-Os analysis of sulfide inclusions in kimberlite olivine: new constraints on depletion events in the Siberian lithospheric mantle. Geochemistry, Geophysics, Geosystems 3 (11), 1069 doi: 10.10292001GC000287.

Griffin, W.L., O'Reilly, S.Y., Abe, N., Aulbach, S., Davies, R.M., Pearson, N.J., Doyle, B.J., Kivi, K., 2003. The origin and evolution of the Archean lithospheric mantle. Precambrian Research 127, 19–41.

Griffin, W.L., Natapov, L.M., O'Reilly, S.Y., van Achterbergh, E., Cherenkova, A.F., Cherenkov, V.G., 2005. The Kharamai kimberlite field, Siberia: modification of the lithospheric mantle by the Siberian Trap event. Lithos 81, 167–187.

Griffin, W.L., Belousova, E.A., O'Neill, C., O'Reilly, S.Y., Malkovets, V., Pearson, N.J., Spetsius, S., Wild, S.A., 2014. The world turns over: Hadean–Archean crust–mantle evolution. Lithos 189, 2–15. http://dx.doi.org/10.1016/j.lithos.2013.08.018.

Grutter, H.S., 2009. Pyroxene xenocryst geotherms: techniques and application. Lithos 112, 1167–1178.

Gudmundsson, G., Wood, B.J., 1995. Experimental tests of garnet peridotite oxygen barometry. Contributions to Mineralogy and Petrology 119, 56–67.

Hart, S.R., Dunn, T., 1993. Experimental Cpx/melt partitioning of 24 trace elements. Contributions to Mineralogy and Petrology 113, 1–8.

Hastie, A.R., Mitchell, S.F., Kerr, A.C., Minifie, M.J., Millard, I.L., 2011. Geochemistry of rare high-Nb basalt lavas: are they derived from a mantle wedge metasomatised by slab melts? Geochimica et Cosmochimica Acta 75, 5049–5072.

Hauri, E.H., Wagner, T.P., Grove, T.L., 1994. Experimental and natural partitioning of Th, U, Pb and other trace elements between garnet, clinopyroxene and basaltic melts. Chemical Geology 117, 149–166.

Horodyskyj, U.N., Lee, C.-T.A., Ducea, M.N., 2007. Similarities between Archean high MgO eclogites and Phanerozoic arc-eclogite cumulates and the role of arcs in Archean continent formation. Earth and Planetary Science Letters 256, 510–520.

Howarth, G.H., Barry, P.H., Pernet-Fisher, J.F., Baziotisa, I.P., Pokhilenko, N.P., Pokhilenko, L.N., Bodnar, R.J., Taylor, L.A., Agashev, A.M., 2014. Superplume Metasomatism: evidence from Siberian mantle xenoliths. Lithos 184–187, 209–224.

Ionov, D.A., Doucet, L.S., Ashchepkov, I.V., 2010. Composition of the lithospheric mantle in the Siberian Craton: new constraints from fresh peridotites in the Udachnaya-East Kimberlite. Journal of Petrology 51, 2177–2210.

Ionov, D.A., Bénard, A., Plechov, P.Yu., Shcherbakov, V.D., 2013. Along-arc variations in lithospheric mantle compositions in Kamchatka, Russia: first trace element data on mantle xenoliths from the Klyuchevskoy Group volcanoes. Journal of Volcanology and Geothermal Research 263, 122–131.

Please cite this article in press as: Ashchepkov, I.V., et al., Comparison of mantle lithosphere beneath early Triassic kimberlite fields in Siberian craton reconstructed from deep-seated xenocrysts, Geoscience Frontiers (2015), http://dx.doi.org/10.1016/j.gsf.2015.06.004

Jolly, W.T., Schellekensb, J.H., Dickinc, A.P., 2007. High-Mg andesites and related lavas from southwest Puerto Rico (Greater Antilles Island Arc): petrogenetic links with emplacement of the Late Cretaceous Caribbean mantle plume. Lithos 98, 1–26.

Karato, S., 2010. Rheology of the Earth's mantle: a historical review. Gondwana Research 18, 17–45.

Kinny, P.D., Griffin, B.J., Heaman, L.M., Brakhfogel, F.F., Spetsius, Z., 1997. Shrimp U–Pb ages of perovskite from Yakutian kimberlites. Russian Geology and Geophysics 38, 97–105.

Klemme, S., Günther, D., Hametner, K., Prowatke, S., Zack, T., 2009. The partitioning of trace elements between ilmenite, ulvospinel, armalcolite and silicate melts with implications for the early differentiation of the moon. Chemical Geology 234, 251–263.

Kogarko, L.N., Ryabchikov, I.D., 2000. Geochemical evidence for meimechite magma generation in the subcontinental lithosphere of Polar Siberia. Journal of Asian Earth Sciences 18, 195–203.

Kostrovitsky, S.I., Morikiyo, T., Serov, I.V., Yakovlev, D.A., Amirzhanov, A.A., 2007. Isotope-geochemical systematics of kimberlites and related rocks from the Siberian Platform. Russian Geology and Geophysics 48, 272–290.

Koulakov, I., Bushenkova, N., 2010. Upper mantle structure beneath the Siberian craton and surrounding areas based on regional tomographic inversion of P and PP travel times. Tectonophysics 486, 81–100.

Kuskov, O.L., Kronrod, V.A., Prokofyev, A.A., Pavlenkova, N.I., 2014. Thermo-chemical structure of the lithospheric mantle underneath the Siberian craton inferred from long-range seismic profiles. Tectonophysics 615–616, 154–166.

Lavrent'ev, Yu. G., Usova, L.V., 1994. New version of KARAT program for quantitative X-ray spectral microanalysis. Zhurnal Analiticheskoi Khimii 5, 462–468.

Leake, B.E., Woolley, A.R., Birch, W.D., Burke, E.A.J., Ferraris, G., Grice, J.D., Hawthorne, F.C., Kisch, H.J., Krivovichev, V.G., Schumacher, J.C., Stephenson, N.C.N., Whittaker, E.J.W., 2003. Nomenclature of amphiboles: additions and revisions to the International Mineralogical Association's amphibole nomenclature. Canadian Mineralogist 41, 1355–1370.

Lee, C.-T.A., Luffi, P., Chin, E.J., 2011. Building and destroying continental mantle. Annual Review of Earth Planetary Sciences 39, 59–90.

Li, X., Zhu, P., Kusky, T.M., Gu, Y., Peng, S., Yuan, Y., Fu, J., 2015. Has the Yangtze craton lost its root? A comparison between the North China and Yangtze cratons. Tectonophysics. http://dx.doi.org/10.1016/j.tecto.2015.04.008.

Logvinova, A.M., Taylor, L.A., Floss, C., Sobolev, N.V., 2005. Geochemistry of multiple diamond inclusions of harzhurgitic garnets as examined in situ. International Geology Review 47, 1223–1233.

Maruyama, S., Sawaki, Y., Ebisuzaki, T., Ikoma, M., Omori, S., Komabayashi, T., 2013. Initiation of leaking Earth: an ultimate trigger of the Cambrian explosion review article. Gondwana Research 25, 910–944. http://dx.doi.org/10.1016/j.gr.2013.03.012.

Mather, K.A., Pearson, D.G., McKenzie, D., Kjarsgaard, B.A., Priestley, K., 2011. Constraints on the depth and thermal history of cratonic lithosphere from peridotite xenoliths, xenocrysts and seismology. Lithos 125, 729–742.

McCammon, C.A., Griffin, W.L., Shee, S.R., O'Neill, H.S.C., 2001. Oxidation during metasomatism in ultramafic xenoliths from the Wesselton kimberlite, South Africa: implications for the survival of diamond. Contributions to Mineralogy and Petrology 141, 287–296.

McDonough, W.F., Sun, S.S., 1995. The composition of the Earth. Chemical Geology 120, 223–253.

McGregor, I.D., 1974. The system $MgO–Al_2O_3–SiO_2$: solubility of Al_2O_3 in enstatite for spinel and garnet–spinel compositions. American Mineralogist 59, 110–190.

McKenzie, D., Priestley, K., 2008. The influence of lithospheric thickness variations on continental evolution. Lithos 102, 1–11.

Mints, M., 2007. Paleoproterozoic supercontinent: origin and evolution of accretionary and collisional orogens exemplified in Northern cratons. Geotectonics 41, 257–280.

Moralev, V.M., Glukhovsky, M.Z., 2000. Diamond-bearing kimberlite fields of the Siberian Craton and the Early Precambrian geodynamics. Ore Geology Reviews 17, 141–153.

Nelson, D.R., Chivas, A.R., Chappel, B.W., McCulloch, M.T., 1988. Geochemical and isotopic systematics in carbonatites and implications for the evolution of ocean island sources. Geochimica et Cosmochimica Acta 52, 1–17.

Nimis, P., Taylor, W., 2000. Single clinopyroxene thermobarometry for garnet peridotites. Part I. Calibration and testing of a Cr-in-Cpx barometer and an enstatite-in-Cpx thermometer. Contributions to Mineralogy and Petrology 139, 541–554.

Nimis, P., Zanetti, A., Dencker, I., Sobolev, N.V., 2009. Major and trace element composition of chromian diopsides from the Zagadochnaya kimberlite Yakutia, Russia): metasomatic processes, thermobarometry and diamond potential. Lithos 112, 397–412.

Nixon, P.H., Boyd, F.R., 1973. Petrogenesis of the granular and sheared ultrabasic nodule suite in kimberlite. In: Nixon, P.H. (Ed.), Lesotho Kimberlites. Cape and Transvaal, Maseru, pp. 48–56.

Nixon, P.H., Boyd, F.R., 1979. Garnet bearing lherzolites and discrete nodules from the Malaita aln6ite, Solomon Islands, S.W. Pacific, and their bearing on oceanic mantle composition and geotherm. In: Boyd, F.R., Meyer, H.O.A. (Eds.), The Mantle Sample: Inclusions in Kimberlites and Other Volcanics. American Geophysical Union, Washington, D.C, pp. 400–423.

O'Neill, H.St.C., Wall, V.J., 1987. The olivine orthopyroxene-spinel oxygen geobarometer, the nickel precipitation curve, and the oxygen fugacity of the Earth's upper mantle. Journal of Petrology 28, 1169–1191.

O'Neill, H.St. C., Wood, B.J., 1979. An experimental study of Fe-Mg-partitioning between garnet and olivine and its calibration as a geothermometer. Contributions to Mineralogy and Petrology 70, 59–70.

O'Reilly, S.Y., Griffin, W.L., 2010. The continental lithosphere–asthenosphere boundary: can we sample it? Lithos 120, 1–13.

Ohara, Y., Stern, R.J., Ishii, T., Yurimoto, H., Yamazaki, T., 2002. Peridotites from the Mariana Trough: first look at the mantle beneath an active back-arc basin. Contributions to Mineralogy and Petrology 143, 1–18.

Pavlenkova, N.I., 2011. Seismic structure of the upper mantle along the long-range PNE profiles — rheological implication. Tectonophysics 508, 85–95.

Pearson, D.G., Shirey, S.B., Carlson, R.W., Boyd, F.R., Pokhilenko, N.P., Shimizu, N., 1995. Re-Os, Sm-Nd, and Rb-Sr isotope evidence for thick Archaean lithospheric mantle beneath the Siberian craton modified by multistage metasomatism. Geochimica et Cosmochimica Acta 59, 959–977.

Pearson, D.G., Snyder, G.A., Shirey, S.B., Taylor, L.A., Carlson, R.W., Sobolev, N.V., 2005. Archaean Re–Os age for Siberian eclogites and constraints on Archaean tectonics. Nature 374, 711–713.

Peslier, A.H., Woodland, A.B., Bell, D.R., Lazarov, M., 2010. Olivine water contents in the continental lithosphere and the longevity of cratons. Nature 467, 78–81.

Pokhilenko, N.P., Pearson, D.G., Boyd, F.R., Sobolev, N.V., 1991. Megacrystalline dunites: sources of Siberian diamonds. Carnegie Institute Washington Yearbook 90, 11–18.

Pokhilenko, N.P., Sobolev, N.V., Kuligin, S.S., Shimizu, N., 1999. Peculiarities of Distribution of Pyroxenite Paragenesis Garnets in Yakutian Kimberlites and Some Aspects of the Evolution of the Siberian Craton Lithospheric Mantle. Proceedings of the VII International Kimberlite Conference. The P.H. Nixon volume, pp. 690–707.

Pokhilenko, N.P., Agashev, A.M., Litasov, K.D., Pokhilenko, L.N., 2015. Carbonatite metasomatism of peridotite lithospheric mantle: implications for diamond formation and carbonatite-kimberlite magmatism. Russian Geology and Geophysics 56, 280–295.

Roberts, N.M.W., Spencer, C.J., 2015. The zircon archive of continent formation through time. In: Roberts, N.M.W. (Ed.), Continent Formation through Time. London, UK, Geological Society of London, Special Publications 389, pp. 197–225.

Rosen, O.M., 1986. The Archean lithosphere as seen in the Anabar shield. International Geology Review 28, 770–783.

Rosen, O.M., 2003. Siberian craton: tectonic zoning, the stages of evolution. Geotectonics 3, 3–21.

Rosen, O.M., Manakov, A.V., Suvorov, V.D., 2005. Collision system at the North East of Siberian craton and problem of diamond grade of lithospheric roots. Geotectonics 6, 42–67.

Rosen, O.M., Levskii, L.K., Makeev, A.F., Zhuravlev, D.Z., Spetsius, Z.V., Rotman, A.Ya., Zinchuk, N.N., Manakov, A.V., Serenko, V.P., 2006. Paleoproterozoic accretion in the Northeast Siberian craton: isotopic dating of the Anabar collision system. Stratigraphy and Geological Correlation 14, 581–601.

Rosen, O.M., Levsky, L.K., Zhuravlev, D.Z., Spetsius, Z.V., Rotman, A.Ya., Zinchouk, N.N., Manakov, A., Serenko, V.P., 2007. The Anabar collision system as an element of the Columbia supercontinent: 600 Ma of compression (2.0–1.3 Ga). Doklady Earth Sciences 417, 1355–1358.

Ryan, C.G., Griffin, W.L., Pearson, N.J., 1996. Garnet geotherms: pressure-temperature data from Cr-pyrope garnet xenocrysts in volcanic rocks. Journal of Geophysical Research Atmospheres 101 (B3), 5611–5625.

Santosh, M., Maruyama, S., Yamamoto, S., 2009. The making and breaking of supercontinents: some speculations based on superplumes, super downwelling and the role of tectosphere. Gondwana Research 15, 324–341.

Shatsky, V.S., Zedgenizov, D.A., Ragozin, A.L., Kalinina, V.V., 2015. Diamondiferous subcontinental lithospheric mantle of the northeastern Siberian Craton: evidence from mineral inclusions in alluvial diamonds. Gondwana Research. http://dx.doi.org/10.1016/j.gr.2014.03.018.

Smelov, A.P., Zaitsev, A.I., 2013. The age and localization of kimberlite magmatism in the Yakutian kimberlite Province: constraints from isotope geochronology—an overview. In: Pearson, D.G., et al. (Eds.), Proceedings of 10th International Kimberlite Conference, Special Issue of the Journal of the Geological Society of India, vol. 1, pp. 225–234.

Smelov, A.P., Andreev, A.P., Altukhova, Z.A., Babushkina, S.A., Bekrenev, K.A., Zaitsev, A.I., Izbekov, E.D., Koroleva, O.V., Mishnin, V.M., Okrugin, A.V., Oleinikov, O.B., Surnin, A.A., 2010. Kimberlites of the Manchary pipe: a new kimberlite field in Central Yakutia. Russian Geology and Geophysics 51, 121–126.

Smith, C.B., Pearson, D.G., Bulanova, G.P., Beard, A.D., Carlson, R.W., Wittig, N., Sims, K., Chimuka, L., Muchemwa, E., 2009. Extremely depleted lithospheric mantle and diamonds beneath the southern Zimbabwe Craton. Lithos 112, 1120–1132.

Smithies, R.H., 2002. Archaean boninite-like rocks in an intracratonic setting. Earth and Planetary Science Letters 197, 19–34.

Sobolev, N.V., 1974. Deep-seated Inclusions in Kimberlites and the Problem of the Composition of the Mantle. American Geophysical Union, Washington, DC, p. 279.

Sobolev, N.V., Lavrentev, Y.G., Pokhilenko, N.P., Usova, L.V., 1973. Chrome-rich garnets from the kimberlites of Yakutia and their Parageneses. Contributions to Mineralogy and Petrology 40, 39–52.

Sobolev, N.V., Yefimova, E.S., Koptil, V.I., 1998. Mineral inclusions in diamonds in the northeast of the Yakutian diamondiferous province. In: Proceedings of the 7th International Kimberlite Conference, Cape Town 2, pp. 616–622.

Please cite this article in press as: Ashchepkov, I.V., et al., Comparison of mantle lithosphere beneath early Triassic kimberlite fields in Siberian craton reconstructed from deep-seated xenocrysts, Geoscience Frontiers (2015), http://dx.doi.org/10.1016/j.gsf.2015.06.004

Stachel, T., Harris, J.W., 2008. The origin of cratonic diamonds — Constraints from mineral inclusions. Ore Geology Reviews 34, 5–32.

Tappe, S., Foley, S.F., Stracke, A., Romer, R.L., Kjarsgaard, B.A., Heaman, L.M., Joyce, N., 2007. Craton reactivation on the Labrador Sea margins: $^{40}Ar/^{39}Ar$ age and Sr-Nd-Hf-Pb isotope constraints from alkaline and carbonatite intrusives. Earth and Planetary Science Letters 256, 433–445.

Taylor, W.R., Kammerman, M., Hamilton, R., 1998. New Thermometer and Oxygen Fugacity Sensor Calibrations for Ilmenite and Chromium Spinel-bearing Peridotitic Assemblages, 7th International Kimberlite Conference. Extended abstracts. Cape town, pp. 891–901.

Taylor, L.A., Snyder, G.A., Keller, R., Remley, D.A., Anand, M., Wiesli, R., Valley, J., Sobolev, N.V., 2003. Petrogenesis of group A eclogites and websterites: evidence from the Obnazhennaya kimberlite, Yakutia. Contributions to Mineralogy and Petrology 145, 424–443.

Tomlinson, E.L., Müller, W., EIMF, 2009. A snapshot of mantle metasomatism: trace element analysis of coexisting fluid (LA-ICP-MS) and silicate (SIMS) inclusions in fibrous diamonds. Earth and Planetary Science Letters 279, 362–372.

Tychkov, N.S., Pokhilenko, N.P., Kuligin, S.S., Malygina, E.V., 2008. Composition and origin of peculiar pyropes from lherzolites: evidence for the evolution of the lithospheric mantle of the Siberian Platform. Russian Geology and Geophysics 49, 225–239.

Williams, H., Hoffman, P.F., Lewry, J.F., Monger, J.W.H., Rivers, T., 1991. Anatomy of North America: thematic portrayals of the continent. Tectonophysics 187, 117–134.

Wittig, N., Pearson, D.G., Webb, M., Ottley, C.J., Irvine, G.J., Kopylova, M., Jensen, S.M., Nowell, G.M., 2008. Origin of cratonic lithospheric mantle roots: a geochemical study of peridotites from the North Atlantic Craton, West Greenland. Earth and Planetary Science Letters 274, 24–33.

Yang, Q.-L., Zhao, Z.-F., Zheng, Y.-F., 2012. Modification of subcontinental lithospheric mantle above continental subduction zone: constraints from geochemistry of Mesozoic gabbroic rocks in southeastern North China. Lithos 146–147, 164–182.

Yu, Y., Xu, X.-S., Griffin, W.L., O'Reilly, S.Y., Xia, Q.-K., 2011. H_2O contents and their modification in the Cenozoic subcontinental lithospheric mantle beneath the Cathaysia block, SE China. Lithos 126 182–197.

Zack, T., Brumm, R., 1998. Ilmenite/liquid partition coefficients of 26 trace elements determined through ilmenite/clinopyroxene partitioning in garnet pyroxenite. In: Gurney, J.J., Gurney, J.L., Pascoe, M.D., Richardson, S.H. (Eds.), 7th International Kimberlite Conference. InRed Roof Design, Capetown, pp. 986–988.

Zaitsev, A.I., Smelov, A.P., 2010. Isotopic geochronology of the kimberlite formations rocks of the Yakutian province. In: Shkodzinsky, V.S. (Ed.), IGMB SO RAN, Yakutsk, p. 107.

Please cite this article in press as: Ashchepkov, I.V., et al., Comparison of mantle lithosphere beneath early Triassic kimberlite fields in Siberian craton reconstructed from deep-seated xenocrysts, Geoscience Frontiers (2015), http://dx.doi.org/10.1016/j.gsf.2015.06.004